ASSAYING PROTEIN IMPORT INTO MITOCHONDRIA USING FLUORESCENCE SPECTROSCOPY

A Thesis

by

HOLLY BETH CARGILL

Submitted to the Office of Graduate Studies of
Texas A&M University
in partial fulfillment of the requirements for the degree of

MASTER OF SCIENCE

May 2006

Major Subject: Biochemistry

ASSAYING PROTEIN IMPORT INTO MITOCHONDRIA USING FLUORESCENCE SPECTROSCOPY

A Thesis

by

HOLLY BETH CARGILL

Submitted to the Office of Graduate Studies of
Texas A&M University
in partial fulfillment of the requirements for the degree of

MASTER OF SCIENCE

Approved by:

Chair of Committee,	Arthur E. Johnson
Committee Members,	George Davis
	Michael Kladde
	J. Martin Scholtz
Head of Department,	Gregory Reinhart

May 2006

Major Subject: Biochemistry

ABSTRACT

Assaying Protein Import into Mitochondria Using

Fluorescence Spectroscopy. (May 2006)

Holly Beth Cargill, B.S., University of Nebraska – Lincoln

Chair of Advisory Committee: Dr. Arthur E. Johnson

Most proteins residing in the mitochondrial matrix are synthesized in the cytosol and post-translationally imported into the mitochondrial matrix. The matrix-targeted preproteins traverse the outer mitochondrial membrane (OM) via the Translocase of the Outer Membrane (TOM) complex, and the inner mitochondrial membrane (IM) via the Translocase of the Inner Membrane 23 (TIM23) complex. A novel system was set up to examine the import of matrix-targeted preproteins into mitochondria using fluorescence spectroscopy. The fluorescent probe 6-(7-nitrobenz-2-oxa-1,3-diazol-4-yl)aminohexanoic acid (NBD) was site-specifically incorporated into different positions along the model matrix protein Su9-DHFR. The fluorescent-labeled polypeptides were either fully imported into isolated mitochondria or were arrested along the translocation pathway by the binding of methotrexate (MTX) to the DHFR moiety, creating NBD-Su9-DHFR•MTX import intermediates. The NBD-Su9-DHFR polypeptides were able to be fully imported into the mitochondrial matrix in the absence of MTX, and were inaccessible to externally-added iodide ion quenchers. Treatment of the mitochondria with the pore-forming antibiotic alamethicin allowed the iodide ion quenchers access to the matrix through pores in the inner membrane (IM). After Alamethicin treatment the

fully-imported NBD-Su9-DHFR polypeptides were accessible to the externally-added iodide ions. The extent of collisional quenching of the NBD fluorophores by the iodide ions was measured as the Stern-Volmer quenching constant, K_{sv}. K_{sv} values were obtained for the NBD-Su9-DHFR polypeptides in the presence of MTX (import intermediates) or in the absence of MTX (fully-imported). The K_{sv} values for NBD-Su9-DHFR import intermediates were similar, despite the location of the NBD probe along the translocation pathway. These K_{sv} values were similar to those obtained for the fully-imported NBD-Su9-DHFR polypeptides (-MTX). The locations of the varying probe positions along the import pathway were addressed using chemical crosslinking of Su9-DHFR Cys mutants. The use of fluorescence spectroscopy, in association with chemical crosslinking, to analyze the mitochondrial protein import pathways will prove a useful tool to probe the environment of the nascent chain as it is crossing the import pathway (the TOM, TIM23 complexes).

To my husband,

Edward

And my children,

Ethan and Caleb

ACKNOWLEDGEMENTS

I would first like to thank my advisor, Dr. Arthur Johnson, for his guidance during my graduate training. Dr. Johnson worked hard to turn me into a scientist who thinks through each experiment prior to actually performing it, and who critically analyzes both the literature and their own data, to accurately interpret the results and better understand the system.

I would like to thank the members of my faculty committee, Dr. J. Martin Scholtz, Dr. George Davis, and Dr. Michael Kladde, for their support and guidance during my graduate career.

I would like to thank my fellow labmates, both graduate students and postdocs, in the Johnson Lab, who have all been supportive and critical at exactly the right times. More specifically, I would like to mention Dr. Alison Davis, who taught me the techniques used in the mitochondrial import field, and Dr. Nathan Alder, who has guided and advised me on the fluorescence experiments. I would also like to thank the Johnson Lab technicians, Yiwei Miao, and Yuan Shao, who synthesized all of the tRNAs necessary for me to complete this project.

I would like to thank the NIH for funding this research project.

Finally, I would like to thank my ever-supportive family: my parents, Nathan and Karen; and my "boys", Edward, Ethan, and Caleb.

TABLE OF CONTENTS

CHAPTER Page

LIST OF FIGURES

FIGURE Page

LIST OF TABLES

CHAPTER I

INTRODUCTION

The Mitochondrion

The mitochondrion is the organelle responsible for energy generation in most eukaryotic cells. Mitochondria are complex organelles, believed to be descendants of a eubacterium that have evolved to become the major cellular source of ATP regeneration through respiration. Unlike most other organelles, the mitochondrial lumen, or matrix, is surrounded by two distinct membranes, termed the outer membrane (OM) and inner membrane (IM). The aqueous space between the OM and IM is called the intermembrane space (IMS) (Figure I-1). The IM is the location for the complexes involved in electron transport, as well as translocators for ATP, NADH, PO_4^{2-}, and many other small molecules. The coupling of electron transport and ATP synthesis generates a proton electrochemical gradient across the IM. To maximize the density of the proteins involved in oxidative metabolism, the IM has a large surface area that is folded into tight cristae, surrounded by the OM.

Mitochondria have long been known to be the site for electron transport and ATP synthesis (IM), the citric acid cycle (matrix), the heme cycle (matrix), and heme biosynthesis (IM, IMS) (Tzagoloff, 1982). The mitochondrion has also been implicated in apoptosis, or programmed cell death (Adrain and Martin, 2001). Mitochondria also

---

This thesis follows the style of Cell.

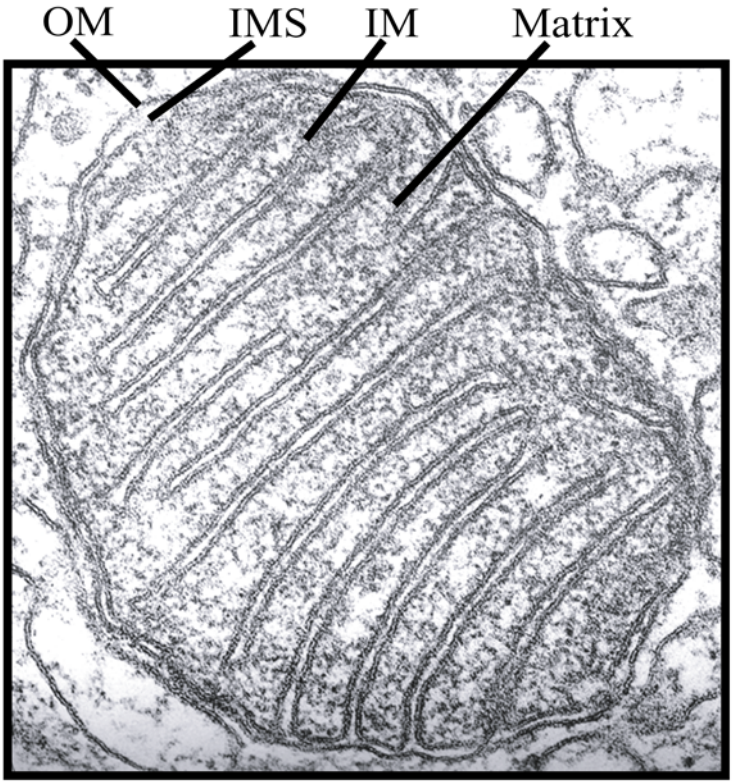

Adapted from Alberts, 3rd. Ed.

Figure I-1. Electron micrograph of isolated mitochondria. OM, outer membrane; IMS, intermembrane space; IM, inner membrane.

contain their own DNA, ribosomes, and translation machinery; however, the genome codes for only eight distinct proteins in yeast, which means that 99% of all mitochondrial proteins are synthesized in the cytosol and imported post-translationally into the organelle (Sickmann et al, 2003).

With all such important metabolic pathways housed in the mitochondrion, the necessity for correct targeting of mitochondrial proteins becomes obvious. To achieve this, mitochondria have multiple import pathways to correctly translocate soluble proteins to the matrix/IMS and to insert a membrane protein into its target membrane (Figure I-2). In addition, cytosolic chaperones aid in delivery of the nascent proteins to the organelle, and help to prevent aggregation of any transmembrane domains prior to insertion. The outer membrane houses the Translocase of the Outer Membrane (TOM) complex, through which nearly all of the imported proteins travel (Kiebler et al, 1990). At this point the pathways diverge. OM β-barrel proteins, such as Tom40p and the yeast porins, are then inserted into the OM via the Sorting and Assembly Machinery (SAM) Complex (Wiedemann et al, 2003). Proteins destined for the IM (often referred to as the carrier proteins) contain internal targeting signals that direct them to the Translocase of the Inner Membrane (TIM) 22 complex for membrane insertion (Truscott and Pfanner, 1999). Matrix-targeted proteins are synthesized in the cytosol with positively charged presequences that direct them to the TIM23 complex (Jensen and Dunn, 2002), where they are translocated across the IM, with the assistance of the Presequence-Assisted Motor (PAM) Complex (Neupert et al, 2003). All of the proteins coded by the mitochondrial genome are IM proteins, inserted into the membrane from the matrix side

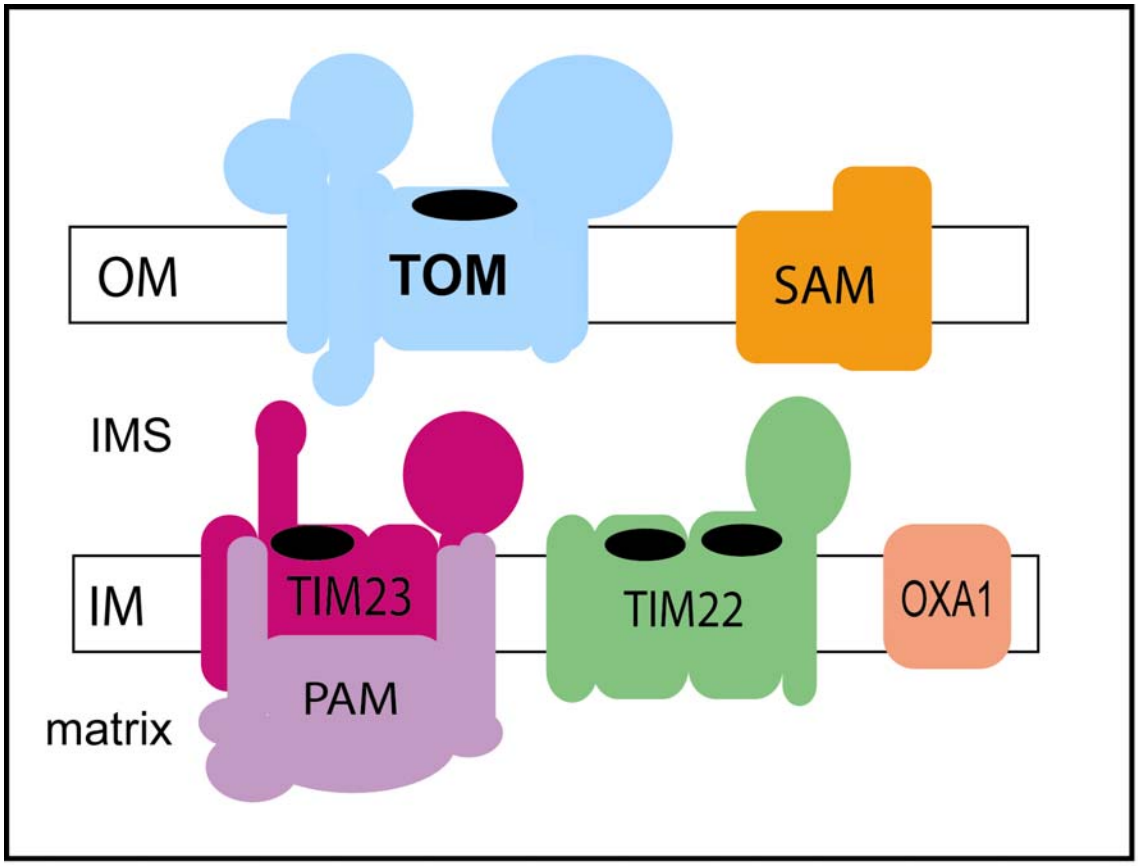

Figure I-2. Protein translocases of the yeast mitchondria. TOM, Translocase of the Outer Membrane; SAM, Sorting and Assembly Machinery; TIM23, Translocase of the Inner Membrane 23 Complex; PAM, Presequence Associated Motor Complex; TIM22, Translocase of the Inner Membrane 22 Complex.

of the IM via the OXA1 complex (Stuart, 2002). Each of these translocation complexes will be discussed in detail below.

The TOM Complex

The TOM complex consists of the proteins Tom40, Tom20, Tom22, Tom70, Tom5, Tom6, and Tom7, all of which are membrane proteins (Figure I-3). Tom40 forms the General Import Pore (GIP) through which almost all proteins targeted to the mitochondria will pass, regardless of their differing targeting signals (Kunkele et al, 1998a; Kiebler 1990; Ahting et al, 1999; Sollner et al, 1992, Hill et al, 1998). Tom40 is believed to form a β-barrel in the OM (Hill et al, 1998; Kunkele et al, 1998a; Ahting et al, 2001), with EM data suggesting that each TOM complex contains 2-3 Tom40 pores (Kunkele et al, 1998b, Achting et al, 1999). Work by Esaki et al (2003) has shown that Tom40 actively participates in transport by binding to incoming preproteins to prevent their aggregation.

The receptor proteins Tom20, Tom22, and Tom70 receive incoming proteins from cytosolic chaperones and transfer them to Tom40. Tom70 is the receptor for IM-targeted proteins, and it has been proposed that each Tom70 monomer binds two IM transmembrane domains (Söllner et al, 1990; Wiedemann et al, 2001). Each Tom70 has specific binding sites for the incoming carrier protein and for the Hsp70 and Hsp90 chaperones that bring the precursor protein to the TOM complex (Young et al, 1993). Tom20 and Tom22 cooperate to bind the matrix-targeted preproteins. Tom20 has been shown to contain a grove consisting of a hydrophobic face designed to bind the

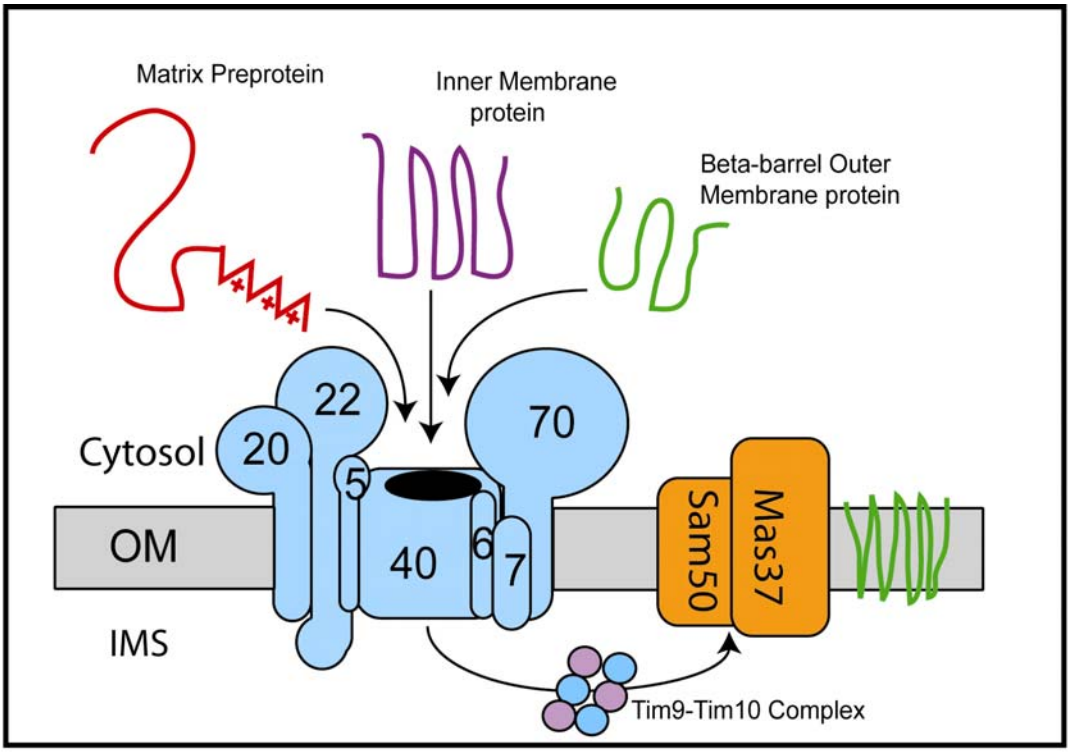

Figure I-3. Protein translocases of the mitochondrial outer membrane (OM). The Translocase of the Outer Membrane (TOM) complex (blue) is comprised of the Tom40 pore, receptors Tom20, Tom22, and Tom70, and single-spanning membrane proteins Tom5, Tom6, and Tom7. The majority of proteins imported into mitochondria, regardless of their target membrane, cross the OM via the TOM complex, including the Beta-barrel OM proteins, which are then inserted into the OM via the Sorting and Assembly Machinery (SAM) complex (orange). The SAM complex consists of the membrane proteins Mas37 and Sam50.

amphipathic α-helix of the matrix targeting presequence, while Tom22 harbors a negatively charged surface to interact with the positively charged surface (Bollinger et al, 1995; Nargang et al, 1998; Abe et al, 2000). In addition, Tom22 also has a negatively charged patch on its IMS domain for binding of the precursor protein after it has passed through the Tom40 pore (Rapaport et al, 1998). The small Tom proteins, Tom5, Tom6, and Tom7, together modulate the structural stability of the TOM complex (Dembowski et al, 2001; Dietmeier et al, 1997; Schmitt et al, 2005).

The SAM Complex

The SAM complex (also referred to as the TOB complex (Paschen et al, 2003)) is the most recently discovered mitochondrial translocase, and is required for insertion of β-barrel proteins into the mitochondrial OM (Figure I-3). The SAM complex was first identified by analyzing the role of Mas37: mitochondria lacking Mas37 are deficient in import of OM β-barrel proteins, such as porin and Tom40, while import of all other mitochondrial proteins proceeds as in the wild-type strain (Wiedemann et al, 2003). More subunits of the SAM complex were later identified, including Sam50 (Tob55/Omp85), Tom13 and Sam35/Tom38 (Kozjak et al, 2003; Paschen et al, 2003; Gentle et al, 2004; Milenkovic et al, 2004; Ishikawa et al, 2004). While the exact mechanism for insertion of β-barrel proteins by the SAM complex is unknown, it appears that these proteins first pass through the Tom40 pore to the IMS, where they are presented to the *trans* side of the membrane for subsequent insertion (Voulhoux et al,

2003). This approach mimics that for protein integration into the bacterial OM, suggesting that this pathway is highly conserved thoughout evolution.

The TIM22 Complex

The TIM22 complex is the pathway used to insert polytopic IM proteins, such as the ADP/ATP Carrier (AAC), the Inorganic Phosphate Carrier (PiC), and Tim23p. Proteins destined for this pathway contain no cleavable targeting sequences, but rather have internal targeting signals that direct them to the TIM22 complex (Wiedemann et al, 2001; Endres et al, 1999; Davis et al, 1998; Davis et al, 2000). The TIM22 complex is made up of inner membrane proteins Tim22, Tim18, and Tim54, as well as the peripheral membrane protein Tim12 (Sirrenberg et al, 1996, Kerscher et al, 1997, Koehler et al, 2000, Kerscher et al, 2000) (Figure I-4). Previous work has shown that polytopic IM proteins traverse the OM in a partially folded conformation, and are then bound in the IMS by small Tim proteins, Tim9•Tim10 and, in some cases (Tim23, for example), Tim8•Tim13 (Koehler et al, 1998; Sirrenberg et al, 1998; Davis et al, 1998; Davis et al, 2000). The Tim9•Tim10 and Tim8•Tim13 complexes then docks with Tim12, delivering the incoming carrier protein to the TIM22 complex. Little is known about the exact roles of Tim18 and Tim54.

Electrophysiological data showed that Tim22 to forms a pore in the IM (Kovermann et al, 2002). Subsequent cryo-electron microscopy work on isolated TIM22 complexes by Rehling et al (2003) revealed that Tim22 forms a “twin-pore” translocase,

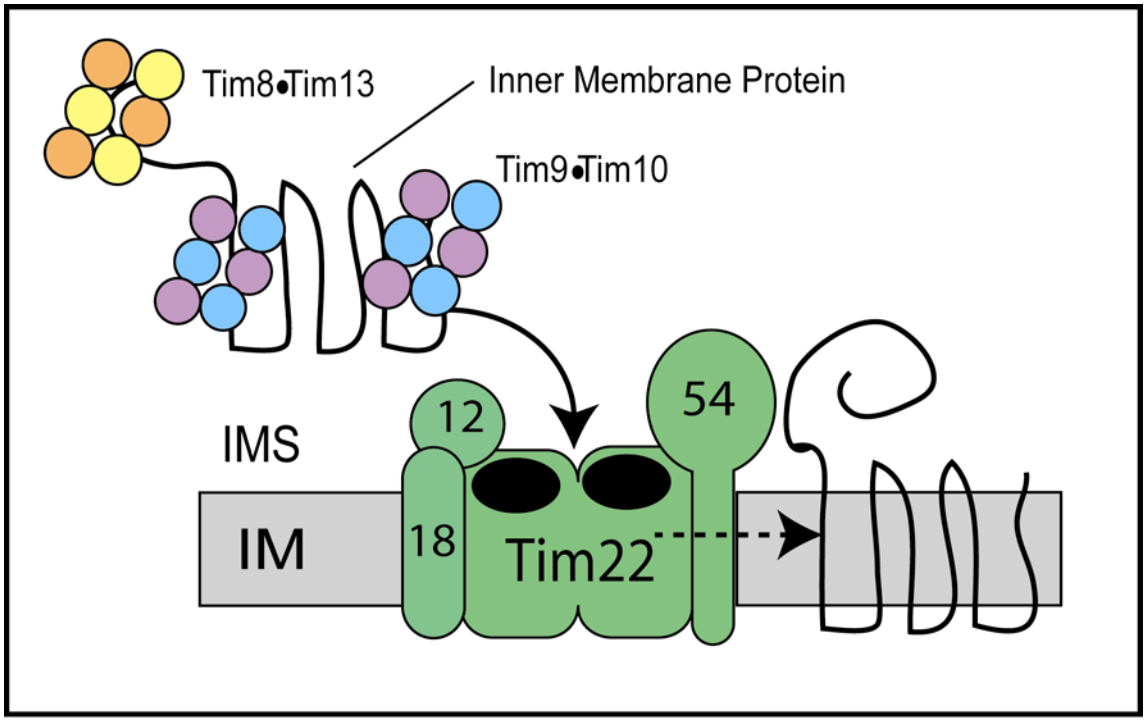

Figure I-4. The Translocase of the Inner Membrane 22 (TIM22) complex. A translocating polytopic IM protein is bound by the Tim9-Tim10 complex, or the Tim8-Tim13 complex, upon entry into the IMS. It is then transferred to Tim12, and subsequently inserted into the pore-forming Tim22, aided by Tim18 and Tim54.

with each pore having an inner diameter of near 16 Å, approximately large enough to allow room for one folded α-helix. The only energy source required for protein insertion via the TIM22 complex is the membrane potential (ΔΨ) across the IM (Pfanner et al, 1985; Pfanner et al, 1987a, b). Further electrophysiology data also revealed that exposure of the internal targeting sequences of the incoming protein to Tim22, in the presence of the ΔΨ, resulted in the rapid closure of one pore and the simultaneous opening of the other, thus appearing to activate the gating of the pores (Rehling et al, 2003).

The small Tim complexes are not directly part of the TIM22 pathway, but have been implicated in the biogenesis of OM β-barrel proteins as well as that of polytopic IM proteins. The Tim9•Tim10 complex has been shown to be essential for import of IM proteins (Koehler et al, 1998a, b; Sirrenberg et al, 1998) while the Tim8•Tim13 complex interacts with IM proteins containing large IMS domains, such as Tim23 (Koehler et al, 1999; Davis et al, 2000). Each of the proteins in these small Tim complexes contains a zinc-finger motif (Curran et al, 2002a, b; Lutz et al, 2003; Allen et al, 2003; Koehler et al, 2004). Their roles then appear to be to guide membrane proteins across the aqueous IMS and prevent aggregation of these proteins prior to insertion. Recent work by Wiedemann et al (2004), and Hoppins et al (2004), has shown the Tim9•Tim10 protein complex to be involved in the biogenesis of OM β-barrel proteins as well, probably by binding to these proteins to prevent their aggregation in the IMS. Import of these small Tim proteins, and likely other resident IMS proteins, appears to be facilitated by Mia40/Tim40 (Chacinska et al, 2004; Naoe et al, 2004, Terziyska et al, 2005). Mia40, in

cooperation with the sulphydryl oxidase Erv1, has been shown to catalyze their import into the IMS (Mesecke et al, 2005).

The TIM23 Complex

The TIM23 complex is the translocase used by matrix-targeted proteins, and by a few IMS and IM proteins. The majority of proteins traveling this pathway are synthesized with an N-terminal, positively charged presequence that is cleaved by matrix processing peptidase (MMP) upon entry into the matrix (for review see Luciano and Geli, 1996). The N-terminal preseqence forms an amphipathic α-helix (Wieprecht et al, 2000; Roise et al, 1998; von Heijne, 1986) that has been shown to be sufficient to direct a protein to the mitochondria (Hurt et al, 1984; Horwich et al, 1985). In addition to the cleaveable presequence, the TIM23 complex also recognizes preproteins containing a hydrophobic signal anchor, for targeting to the IM, as well as proteins containing a bipartite presequence that consists of a matrix presequence followed by a hydrophobic sorting signal, for targeting to the IMS (Glick et al, 1992; Hahne et al, 1994; Gartner et al, 1995, Schneider et al, 1991; Nunnari et al, 1993).

The TIM23 complex is made up of four essential IM proteins: Tim23, Tim17, Tim50, and Tim21 (Figure I-5). Electrophysiological experiments on purified Tim23 have indicated that it is the pore-forming subunit of the TIM23 complex, with an aqueous pore of between 13 and 24 Å wide (Truscott et al, 2001). These experiments support earlier data by Schwartz and Matousek (1999) that attempted to address the pore size of the TIM23 complex using 19 and 26 Å gold particles attached to model matrix

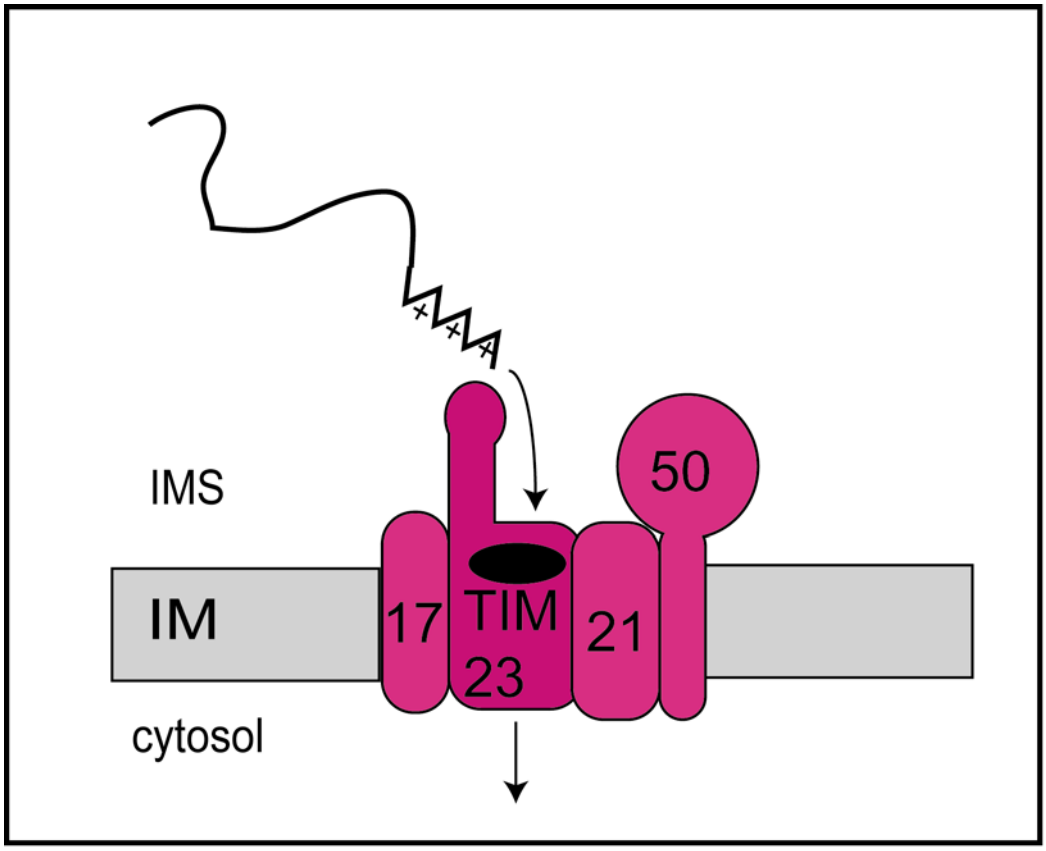

Figure I-5. The Translocase of the Inner Membrane 23 (TIM23) complex. The TIM23 complex functions to import matrix preproteins, containing a positively-charged presequence, into the matrix. The TIM23 complex is comprised of four membrane proteins Tim23, the putative pore-forming subunit, Tim17, Tim21, and Tim50.

proteins, and found that only the 19 Å gold particles could be successfully imported into the matrix. Tim23 is composed of two domains: an N-terminal domain that resides in the IMS, and a C-terminal domain composed of four transmembrane α-helices that resides in the IM (Dekker et al, 1993; Emtage and Jensen, 1993). The C-terminal domain is the pore-forming domain, while the N-terminal domain modulates interactions with the incoming presequences (Bauer et al, 1996; Truscott et al, 2001). Tim17 is structurally similar to the C-terminal domain of Tim23, but cannot complement a Tim23 deletion (Maarse et al, 1994, Ryan et al, 1994). Tim21 and Tim50 both have single transmembrane segments, and Tim50 also has a large IMS domain that interacts with incoming matrix presequences (Chacinska et al, 2005, Mokranjac et al, 2005, Mokranjac et al, 2003, Geissler et al, 2002, Yamamoto et al, 2002). Tim21 appears to modulate the functionality of the TIM23 complex, and will be discussed in more detail below.

While it is possible to directly import matrix-targeted preproteins across the IM in the absence of the OM and TOM complex (termed mitoplasts; Hwang et al, 1989), it is generally believed that the TOM complex and TIM23 complex form a translocase contact site through which the matrix proteins travel (Dekker et al, 1997; Donzeau et al, 2000). There are patches of negatively-charged residues on the *cis* and *trans* side of Tom22, as well as Tim50, that appear to interact with the positively-charged side of the N-terminal presequence, driving translocation across the OM and to the *cis* side of the TIM23 complex (Bollinger et al, 1995). This phenomenon of protein translocation via interactions of a positively-charged protein domain with proteins of increasing negative charges is referred to as the acid chain hypothesis (Schatz et al, 1996). After

translocation across the OM, the presequence is believed to trigger opening of the Tim23 pore by an interaction with its IMS domain (Bauer et al, 1996, Truscott et al, 2001). The presequence then crosses the IM in a $\Delta\Psi$-dependent manner, where it is pulled across the IM and into the matrix by the PAM complex, which will be described below (Pfanner et al, 1987a; Martin et al, 1991; Kanamori et al, 1999).

Tim21 is the most recently discovered subunit of the TIM23 complex. It appears to bind to the *trans* side of Tom22, further linking the TOM and TIM23 complexes (Chacinska et al, 2005, Mokranjac et al, 2005). After the incoming presequence binds to Tom22, Tim21 dislodges the presequence and allows it to be transferred to the Tim23 channel (Chacinska et al, 2005). This occurs because Tim21 completes with the same binding site on Tom22 as the incoming preprotein. An extension of this work found that Tim21 appears to then disassociate from the TIM23 complex, allowing for association of the PAM channel and subsequent translocation of the entire preprotein across the IM. Binding of both Tim21 and the PAM Complex to the TIM23 complex appears to occur through Tim17 and both likely compete for the same binding site (Chacinska et al, 2005, Murcha et al, 2005).

The discovery of these two different states of TIM23 (Tim21 bound or PAM bound) brings forward a means of separating the protein translocation and protein insertion functions of the TIM23 complex. While Tim21 is bound and PAM is not bound (or is more loosely associated), protein translocation cannot occur, setting up an ideal situation for protein insertion, which is a much less studied aspect of the TIM23 complex.

The PAM Complex

The PAM complex associates with the TIM23 complex during protein translocation and functions to pull the incoming matrix preprotein across the IM and into the matrix. It consists of the peripheral membrane protein Tim44, the chaperone mtHsp70/Ssc1 and its nucleotide exchange factor Mge1, and three co-chaperones Pam16, Pam17, and Pam18/Tim14 (Figure 1-6). Tim44 interacts with both Tim23 and mtHsp70, and is believed to recruit the matrix chaperone to the TIM23 complex so that it can exert its pulling effect on the incoming preprotein (Schneider et al, 1994, Merlin et al, 1999, Moro et al, 2002; D'Silva et al, 2003, D'Silva et al, 2004). The ability of mtHsp70 to pull the incoming preprotein across the IM requires successive rounds of ATP-hydrolysis, assisted by Pam16, Pam18, and Mge1. Pam18, being a member of the J domain family, stimulates the ATPase activity of mtHsp70, while Pam16 helps to recruit Pam18 to the TIM23 complex, keeping the PAM complex near the presequence translocase (Truscott et al, 2003; D'Silva et al, 2003; Kozany et al, 2004; Frazier et al, 2004). Pam17, the most recently discovered subunit of the complex, appears to be required for association of Pam16 and Pam18 with the TIM23 complex (van der Laan et al, 2005).

Ssc1, being a member of the heat shock protein family, contains two separate domains, a peptide binding domain and a nucleotide-binding domain (Craig et al, 1989). In the presence of ATP, Ssc1 has a high affinity for both the presequence and Tim44,

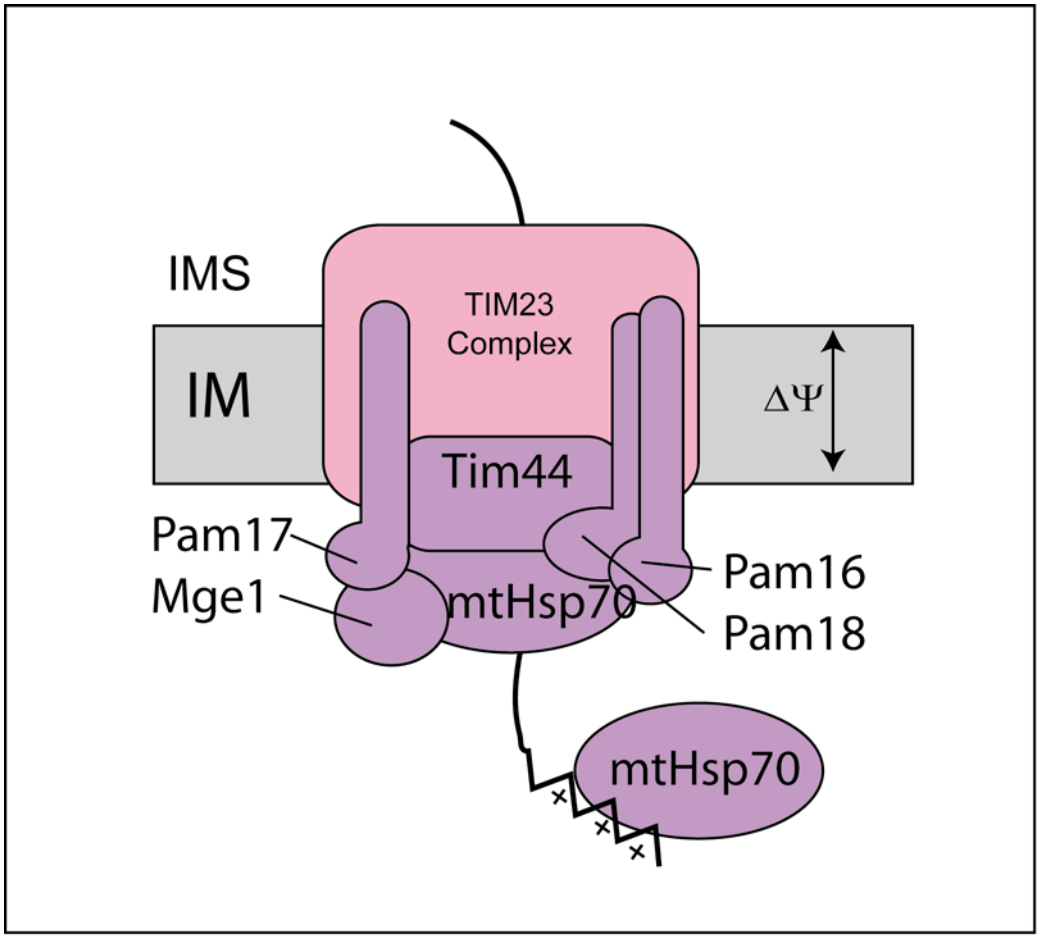

Figure I-6. The Presequence Associated Motor (PAM) complex. The PAM complex consists of the peripheral membrane protein Tim44, mtHsp70, its nucleotide exchange factor Mge1, and three single-spanning membrane proteins Pam16, Pam17, and Pam18. After the matrix preprotein crosses the IM via the TIM23 complex, the protein is pulled into the matrix by mtHsp70, which, depending on the state of its nucleotide (ADP or ATP) can be found associated with either Tim44 and the preprotein, or with the preprotein alone.

which allows the chaperone to be in the proper position on the matrix side of the TIM23 channel to bind the translocating preprotein (Schneider et al, 1994; Moro et al, 2002; Strub et al, 2002; D'Silva et al, 2004). This binding of the preprotein by mtHsp70 results in dissociation from Tim44, which causes Ssc1 to dislocate from the TIM23 complex (Geissler et al, 2001; Liu et al, 2003). The "free" Ssc1 molecule takes with it the incoming polypeptide, bound tightly enough to prevent retrograde translocation back into the channel (Ungermann et al, 1994; Ungermann et al, 1996). An exchange of ADP for ATP by the nucleotide exchange factor Mge1 would then allow mtHsp70 to dissociate from the substrate polypeptide. Dislocation of one Ssc1 molecule from the TIM23 complex allows for a second molecule to bind the next segment of the incoming polypeptide, repeating the cycle until the polypeptide is transported entirely across the IM and into the matrix.

Much of the early literature concerning Ssc1 centered on whether the action of mtHsp70 on the incoming preprotein constitutes a "trapping" or "pulling" force. However, it has since been discovered that both roles can be given to the chaperone. Binding of the presequence by mtHsp70 can be considered a "trapping" force, in that it prevents diffusion of the matrix preprotein back up into the cytosol. Dislocation of the peptide-bound mtHsp70 away from the TIM23 complex comprises a "pulling" force in that it physically draws the peptide further into the matrix. These separate roles can be described to separate functions of Ssc1: interaction of mtHsp70 with the preprotein via the Ssc1 peptide-binding domain, and interaction with the membrane anchor Tim44.

Mutations in these different domains of mtHsp70 appear to modulate the two functions distinctly (Voisine et al, 1999).

The OXA Complex

The OXA complex is located in the IM, and serves to insert inner membrane proteins from the matrix side of the IM. The Oxa1 protein (to date the only known protein of the complex) was originally discovered as being required for formation of cytochrome c oxidase (part of Complex IV of the electron transport chain) (Bonnefoy et al, 1994; Bauer et al, 1994). Most of the proteins inserted into the IM via Oxa1 are those translated on mitochondrial ribosomes, although some nuclear-encoded proteins are also inserted via this pathway (Hell et al, 1997, 1998, 2001). The Oxa1 protein is a member of the Oxa1/YidC/Alb3 family, and appears to function as a dimer or tetramer (Nargang et al, 2002). Consistent with other members of the family, Oxa1 has been shown to cotranslationally insert polytopic proteins into the IM, although some IM-targeted proteins translated on cytosolic ribosomes are also inserted post-translationally (for review see Stuart, 2002).

Current Dogma for Import of Matrix-Targeted Proteins

Translocation of matrix preproteins is the most well studied pathway of mitochondrial import. Matrix protein import is believed to be post-translational (Jensen and Dunn, 2002), unlike proteins of the ER secretory pathway (for review, see van Waes and Johnson, 1999). In accordance with current data, the import pathway functions as

follows: The positively charged presequence directs the protein to the mitochondria, aided by cytosolic chaperones, where it engages the TOM complex via the Tom22/Tom20 receptors and is subsequently passed through the Tom40 pore. Once the preprotein reaches the IMS, the presequence binds to the IMS domain of Tom22 and then moves to the IMS domains of the Tim50 and Tim23. Binding of the presequence to the N-terminal domain of Tim23 results in activation of the Tim23 pore. In a $\Delta\Psi$-dependent manner, the presequence crosses the IM via the Tim23 pore and is then bound by mtHsp70. Through successive rounds of ATP hydrolysis, aided by the other members of the PAM complex, the entire preprotein is pulled across the IM by the mtHsp70 protein, where the mitochondrial processing peptidase (MPP) then cleaves the presequence and the matrix chaperones fold the protein into its final conformation (for a review on MPP see Gakh et al, 2002). Removal of the presequence allows the mature portion of the matrix protein to be folded, with the aid of chaperones, into its active conformation (Figure I-7).

As well studied as the pathway is, there are many questions left unanswered. While it has been shown that TOM/TIM supercomplexes are formed during the import of a matrix preprotein (Dekker et al, 1997), it is as yet unknown whether the preprotein is ever exposed to the aqueous IMS. The Tim23 protein has also been shown to be the pore-forming subunit of the TIM23 complex, containing an aqueous pore (Truscott et al, 2001), but it has not been shown experimentally whether a translocating preprotein passes through the IM via this aqueous pore. It is also unkown how the Tim23 pore is

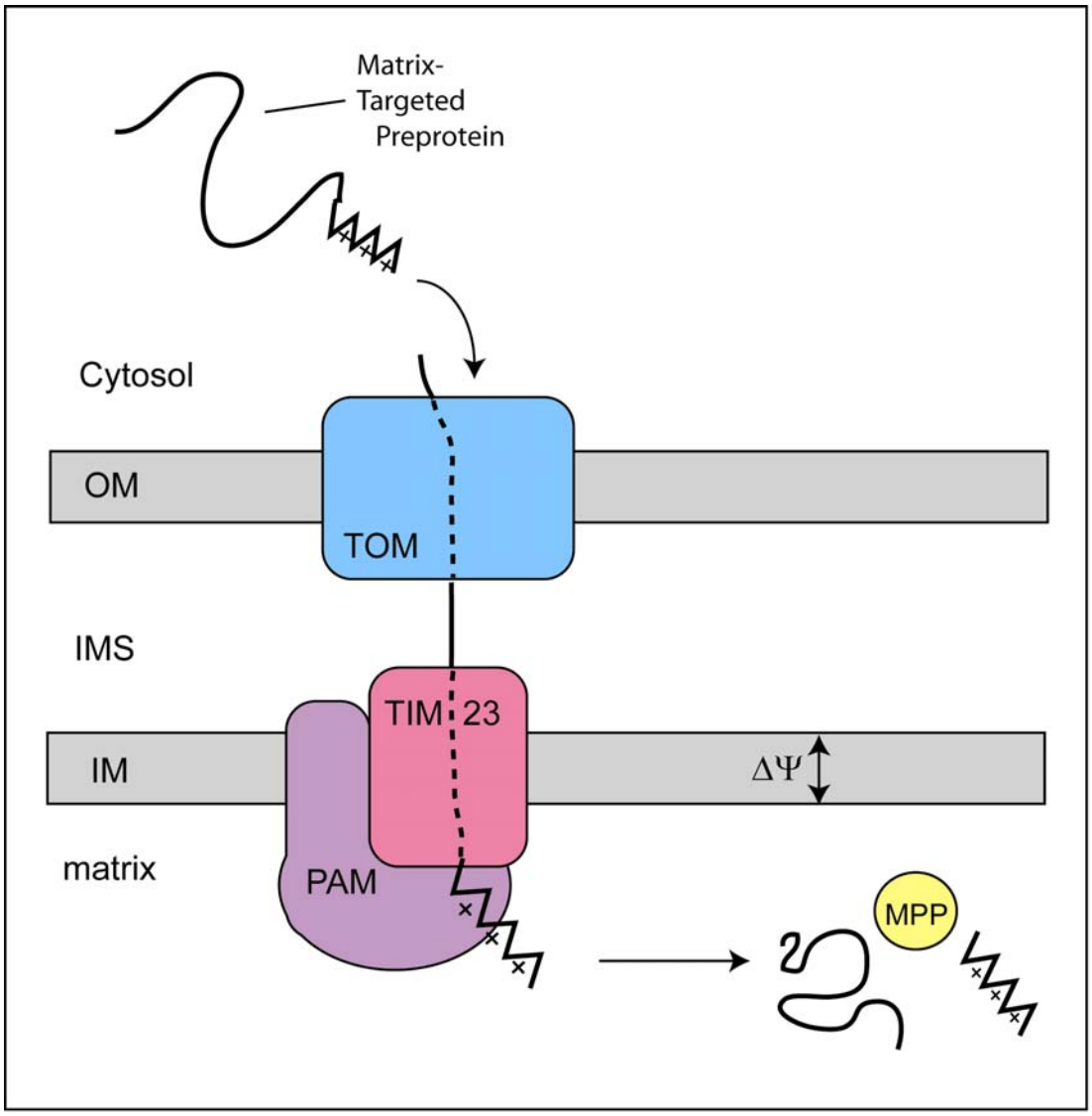

Figure I-7. Import pathway for a matrix preprotein. A matrix preprotein, containing a positively-charged presequence, traverses the OM through the TOM complex. It then crosses the IM via the TIM23 complex, in association with the PAM complex. MPP cleaves the presequence, and the protein is then folded by matrix chaperones into its mature conformation.

gated during translocation, although this is required to maintain the membrane potential. Indeed, membrane depolarization blocks ATP production by the mitochondrion.

Each of these questions can be addressed with a fluorescence-based system. By site-specifically labeling a matrix preprotein with fluorescent probes and generating import intermediates it would be possible to ascertain the environment of the translocating preprotein as it is crossing the OM and IM.

Specific Aims of This Thesis

The primary goal of this research project was to develop a fluorescence-based system to study protein import into mitochondria. Previously in the lab, the translocation of secretory proteins across the ER membrane was examined using a fluorescence-based system whereby nascent secretory proteins (i.e., still attached to the translating ribosomes) were site-specifically labeled with fluorescent probes (Crowley et al, 1994; Hamman et al, 1997). These fluorescent ribosome•nascent chain complexes (RNCs) were co-translationally targeted to translocons in the ER membrane to form translocation intermediates. Using this approach, the environment and accessibility of the fluorophore to different sides of the ER membrane was characterized while the nascent chain was positioned within and interacting with the translocation machinery. Different stages of translocation were investigated by shortening or lengthening the nascent chain, and different portions of the nascent chain were examined.

Would it be possible to site-specifically label a matrix-targeted protein with a fluorescent probe, import the labeled proteins into isolated mitochondria, and analyze the

fluorescence signal of the imported proteins? If so, my original goals were to: (i) determine whether the imported polypeptide is exposed to the aqueous IMS; (ii) whether it passes through an aqueous pore in the TIM23 complex; and (iii) if so, bow the the IM maintains its permeability barrier during protein import into the matrix. While the difficulties of successfully created and characterizing this new experimental system prevented me from achieving these goals, the progress towards the goals described in this thesis provides the foundation upon which to build and determine those unknowns.

CHAPTER II

EXPERIMENTAL PROCEDURES

Preparation of Lys-tRNA^{amb}

A plasmid encoding the wild-type *Escherichia coli* (*E. coli*) lysine tRNA gene, a gift from Dr. Greg Beckler (Promega, Madison, WI), was used for site-directed mutagenesis to change the anticodon loop to CUA, creating an amber suppressor tRNA (here termed tRNA^{amb}). PCR was performed to amplify the region of the plasmid that contained the T7 promoter sequence and the in-frame amber suppressor tRNA gene. An *in vitro* transcription reaction was performed, using the purified PCR products and T7 RNA polymerase, and incubated at 37°C for at least 4 h. The resulting tRNA was purified by anion exchange chromatography using a Mono Q HR 10/10 column on an FPLC (Pharmacia). The tRNA was eluted in 10 mM NaOAc (pH 4.5), 5 mM $MgCl_2$ with a 115 mL linear gradient of NaCl from 480 mM to 1 M. Aminoacylation was performed to determine which fractions were enriched in tRNA^{amb} as described previously (Crowley et al, 1993; Johnson et al, 1982; Krieg et al, 1989; Krieg et al, 1986) with the modification that 6 mM $MgCl_2$ and no KCl was used. The majority of the tRNA eluted near 550 mM NaCl and the fractions with the highest functional tRNA^{amb} content were aminoacylated with [^{14}C]Lys and stored at –80°C until needed (Flanagan et al, 2003).

Chemical Modification of [^{14}C]Lys-tRNA^{amb}

The side chain amino group of lysine in [^{14}C]Lysine-tRNA^{amb} was preferentially reacted with the succinimidyl ester of 6-(7-nitrobenz-2-oxa-1,3-diazol-4-yl)aminohexanoic acid (NBD) to form N$^{\varepsilon}$-NBD-Lys-tRNA^{amb} (εNBD-Lys-tRNA^{amb}) as previously described (Johnson et al, 1976; Crowley et al, 1993). The resultant modified [^{14}C]Lys-tRNA^{amb} was purified and its specific activity measured, expressed in units of pmol Lys/A_{260} units of tRNA . The structure of εNBD-[^{14}C]Lys tRNA^{amb} is shown below (Figure II-1).

Preparation of Yeast Mitochondria

The *Saccharomyces cerevesiae* yeast strain D273-10B was a generous gift from Dr. Rob Jensen (Johns Hopkins University, Baltimore, Maryland). The mitochondrial isolation protocol was modified from a protocol from Daum et al (1982). To increase the amount of mitochondria per OD_{600} of yeast culture, the yeast were grown in media containing lactate as the major sugar source (referred to as SSlac media). Under these conditions, the yeast are forced to activate the citric acid cycle for energy generation. The enzymes involved in the citric acid cycle are contained in the mitochondrial matrix; therefore, up-regulation of the citric acid cycle will result in an increase in the amount of mitochondria per yeast cell. Before a mitochondrial isolation was performed, yeast cells from the D273-10B strain were streaked onto YEPlac (yeast extract, peptone, 20% Na-

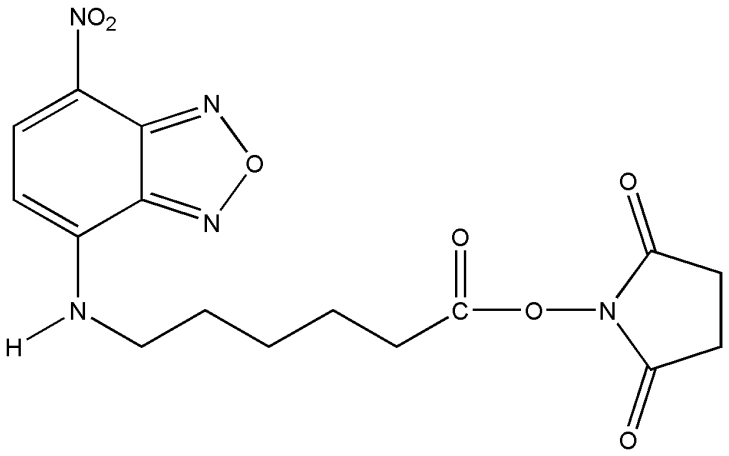

6-(7-nitrobenz-2-oxa-1,3-diazol-4-yl)-aminohexanoyl ester of N-hydroxy-succinimide

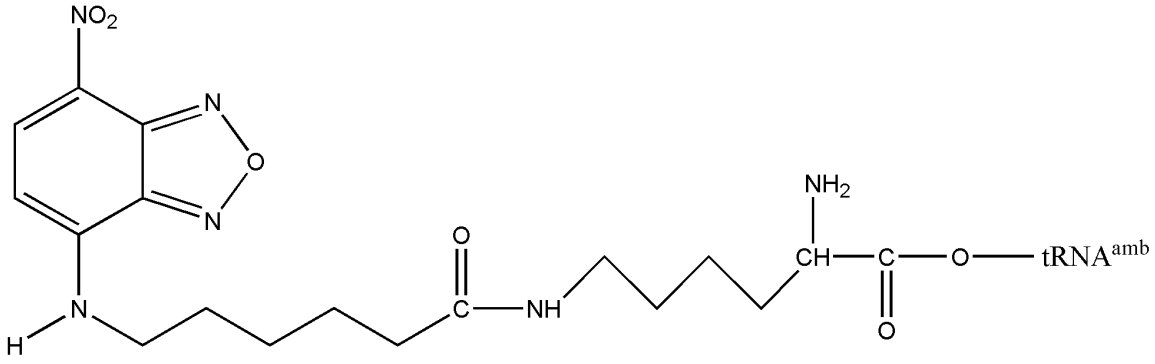

N^{ε}-(6-(7-nitrobenz-2-oxa-1,3-diazol-4-yl)-aminohexanoyl)-Lys-$tRNA^{amb}$
εNBD-Lys-$tRNA^{amb}$

Figure II-1. Structures of the succinimidyl ester of NBD and of εNBD-Lys-$tRNA^{amb}$.

lactate, pH 5.5, and agar) plates, and allowed to sit out at room temperature for 5-7 days. During that time stock solutions for the isolation procedure were made. To make the 20% Na-lactate (pH 5.5), 235 mL of 85% lactic acid (EM, LX0020-6) was added to 500 mL H_2O, and then solid NaOH pellets were added (while the beaker was cooled with ice) until the pH reached 5.5. The volume was adjusted to 1 L with H_2O and autoclaved. For 1 L 5X SSlac media, 15 g of yeast extract, 5 g of KH_2PO_4, 5 g of NH_4Cl, 2.5 g of NaCl, 2.5 g of $CaCl_2$, 3 g of $MgCl_2$, and 2.5 g of glucose were added to 500 mL of Na-lactate (pH 5.5) and the volume was adjusted to 1 L with H_2O before autoclaving. To make 1X SSlac, the 5X SSlac was diluted 1 to 5 with autoclaved H_2O. Three days before the prep, a starter culture containing 5 mL 1X SSlac and a swatch of yeast from the YEPlac plate was incubated at 30°C overnight with shaking (250 rpm). The next day, 100 mL of 1X SSlac, containing the 5 mL of starter culture from the previous night, was incubated at 30°C overnight, with shaking, and the OD_{600} was recorded the next morning when the culture was removed from the incubator.

A volume of the 100 mL starter culture was added to each of two 4 L beakers, containing 2 L pf 1X SSlac, such that the OD_{600} of each 2 L culture was around 0.0625. When the cultures were grown with lactate as the sugar source, the doubling time (i.e., the time required for the OD_{600} to increase by a factor of 2) was around 3 hours. Therefore, after the 2 L cultures were incubated at 30°C with shaking for 12 hours, the OD_{600} was between 1-2. Once the OD_{600} was at or above 1.0, the cells were harvested by sedimentation at 5,000 RPM, 4°C, for 5 min (Beckman JA-10 rotor), and the media was discarded. The cell pellets were then washed with double-distilled water (ddH_2O) (200

mL for a cell pellet from a 2 L culture), centrifuged (at 5,000 RPM, 4°C, 5 min in a Beckman JA-14 rotor), and the mass of each wet cell pellet was noted. The pellets were resuspended in 0.1 M Tris-SO_4 (pH 9.4)/10 mM DTT at 1 mL buffer/0.3 g cells.

All resuspensions after this point were done using gentle swirling of the pellet in the solution, as opposed to resuspension using glass pipettes, in order to maintain the integrity of the mitochondrial membranes. The resuspended pellets were incubated at 30°C for 15 min with slow shaking (125 RPM), then centrifuged as above. The pellets were then resuspended in 100 mL of 1.2 M sorbitol/20 mM KPO_4 (pH 7.4) and centrifuged as above. During the sedimentation a 1 mg/mL solution of Zymolyase 20T (ICN) was made in the sorbitol/KPO_4 buffer.

The cell pellets were then resuspended in the sorbitol/KPO_4 buffer at a volume of 1 mL/0.15 g cell pellet. The Zymolyase solution was added to a concentration of 2 mg per gram cell pellet, and the cells were incubated at 30°C for 30 minutes, to allow the Zymolyase to permeate the yeast cell wall and generate spheroplasts. After 30 min, the cells were centrifuged at 3500 RPM, 5 min, 4°C (Beckman JA-14 rotor), and the supernatant was carefully poured away from the loose pellets. The pellets were gently resuspended in 30 mL 1.2 M sorbitol (usually the pellets were mixed into the sorbitol with a pipette bulb before swirling to finish the resuspension) and centrifuged for 5 min, 3500 RPM, 4°C (Beckman JA-14 rotor). This step was repeated two more times, then the pellets were resuspended in ice-cold SEH buffer (250 mM sucrose, 1 mM EDTA, 20 mM HEPES (pH 7.4), containing 0.5% (w/v) BSA and 1 mM PMSF (as well as 1 μg/mL of both aprotinin and leupeptin) at a volume of 2 mL per gram of cells.

The resuspension was transferred to a 15 mL Pyrex dounce homogenizer and homogenized with 15 strokes using pestle "B". The homogenate was then poured into a 50 mL centrifuge tube, and the dounce was rinsed with an equal volume of SEH buffer. This rinse was added to the homogenate, which was then centrifuged 5 min., 3500 RPM, 4°C (Beckman JA-17 rotor). The supernatant (containing the mitochondria) was transferred to a clean 50 mL centrifuge tube, and the homogenization step was repeated a second time with the pellet (which contained unbroken cells and nuclei). After the homogenization step was repeated, the supernatants from the two sedimentation steps were combined and then centrifuged at 10,000 RPM, 4°C, for 10 min (Beckman JA-17 rotor).

The supernatant was poured off and the pellets (containing the crude mitochondrial fraction) were resuspended in 30 mL SEH buffer and centrifuged at 3000 RPM, 4°C, for 5 min (Beckman JA-17 rotor). The supernatants were transferred to clean 50 mL centrifuge tubes and then centrifuged at 10,000 RPM, 4°C, for 10 min (Beckman JA-14 rotor). The supernatant was removed and the last two steps were repeated once more with the mitochondrial pellets. After the second spin at 10,000 RPM, the isolated mitochondria were resuspended in 0.5 mL SEH buffer (lacking protease inhibitors) and kept on ice. The yield of mitochondria was calculated by adding 10 μL mitochondria to 1 mL of 0.6% (w/v) SDS and reading the A_{280} of the sample (as a blank for the spectrophotometer, 10 μL of SEH buffer was added to 1 mL of 0.6% (w/v) SDS). The resulting A_{280} reading was then put into the following equation to calculate the yield of mitochondrial protein:

$$\frac{0.21}{10\ \text{mg/mL}} = \frac{A_{280}}{C\ \text{mg/mL}} \qquad (1)$$

where C = the concentration of the prepped mitochondria. By multiplying the concentration, C, by the volume in mL of the prep the total mitochondrial protein in mg could be determined. The mitochondria were split into 0.5 mg aliquots and frozen with liquid nitrogen, then stored at –80°C. The frozen mitochondria would generally be stable for 2-3 months.

Site-Directed Mutagenesis

DNA primers were synthesized commercially and ordered from either Integrated DNA Technologies (IDT) or Sigma-Genosys. Primers were resuspended in ddH_2O to a stock concentration of 50 pmol/μL. A working stock of each primer was then made to a concentration of 125 ng/μL. A typical PCR reaction contained the following: 1X Pfu buffer (Stratagene), 200 μM of each dNTP, 2 mM $MgCl_2$, 2.5 ng each of the forward and reverse primers, 50 ng template DNA, and water to adjust the volume to 50 μL, then 0.5 μL of 2.5 U/μL Pfu polymerase (also from Stratagene) was added. The thermal cycler conditions are as follows: initial heating to 95°C for 30 sec, then 20 cycles of denaturing at 95°C for 30 sec, annealing at 55°C for 1 min., and elongation at 68°C for 7 min, followed by cooling the reaction to 4°C.

After the PCR reaction was finished, 2 μL of 10 U/μL DpnI (Promega) was added to each tube, and the reactions were incubated at 37°C for 1-2 hours. The treated reaction (1 μL) was added to 50 μL competent *E. coli* cells (MC1061 or Top10 cells

(Invitrogen)) and allowed to incubate on ice for 15 minutes. The cells were heat-shocked at 42°C for 60 seconds, then cooled again on ice for 2 min. SOC or LB media (450 μL) were added to the cells, and the reaction was incubated at 37°C with shaking (250 rpm) for 1 hour. Cells (100 μL) were then spread onto LB plates containing 50 – 100 μg/mL ampicillin, and the plates were incubated overnight at 37°C before being stored at 4°C. Colonies were picked, and plasmid DNA was isolated using a QiaSpin miniprep kit. Aliquots of the plasmid DNA were sent to the DNA Technologies Lab (College of Veterinary Medicine, Texas A&M) for sequencing. Typically, the primer 1166-HC was used as the sequencing primer. The rest of the purified plasmid DNA was stored at –20°C.

Table II-1 lists all of the primers used to make the mutations necessary for this thesis. The naming of the primers follows that adopted by the Johnson lab, where each primer is assigned the next number in the sequence, followed by the initials of the person who ordered the oligo.

Table II-1. Primers for site-directed mutagenesis of Su9-DHFR constructs

Name	Sequence	Complement	Mutation
227-HC	GCTCAGGTCAGCTAGCGCACCATCCAGACTGGC	228-HC	K33 -> TAG
228-HC	GCCAGTCTGGATGGTGCGCTAGCTGACCTGAGC	227-HC	K33 -> TAG
229-HC	CCTCTTCAGTGGAAGGTTAGCAGAACCTGGTGATTATGGG	230-HC	K119 -> TAG
230-HC	CCCATAATCACCAGGTTCTGCTAACCTTCCACTGAAGAGG	229-HC	K119 -> TAG
231-HC	GTTCTCAGTAGAGAGCTCTAGGAACCACCACCAGG	232-HC	K153 -> TAG
232-HC	CCTCGTGGTGGTTCCTAGAGCTCTCTACTGAGAAC	231-HC	K153 -> TAG
233-HC	GATTTGGGGAAATATTAGCTTCTCCCAGAATACCCAGGC	234-HC	K230 -> TAG
234-HC	GCCTGGGTATTCTGGGAGAAGCTAATATTTCCCCAAATC	233-HC	K230 -> TAG
237-HC	GCCACCACCCGCCAGTAGTTCCAGAAGCGCGCCTAC	238-HC	A61 -> TAG
238-HC	GTAGGCGCGTTCTGGAACTACTGCGCGGTGGTGGC	237-HC	A61 -> TAG
239-HC	CTCAAGCGCACCCAGTAAGAGCTCCATCGTCAAC	240-HC	M50 -> TAG
240-HC	GTTGACGATGGAGCTCTACTGGGTTGAACTGCATC	239-HC	M50 -> TAG
241-HC	GACGGCATCATGGTTTAGCCGTTGAACTGCATC	242-HC	R75 -> TAG
242-HC	GATGCAGTTCAACGGCTAAACCATGATGCCGTC	241-HC	R75 -> TAG
255-HC	CGCGCCTACTCTTCCTAGGGCATCATGGTTCGACC	256-HC	D70 -> TAG
256-HC	GGTCGAACCATGATGCCCTAGGAAGAGTAGGCGCG	255-HC	D70 -> TAG
285-HC	CCGACGGCATCTAGGTCCGACCATTGAACTGC	286-HC	M73 -> TAG
286-HC	GCAGTTCAATGGTCGGACCTAGATGCGTCGG	285-HC	M73 -> TAG
621-HC	GCCTCCACTCGTGTCCTCTAGTCTCGCCTGGCCTCC	622-HC	A8 -> TAG
622-HC	GGAGGCCAGGCGAGACTAGAGGACACGAGTGGAGGC	621-HC	A8 -> TAG
689-HC	GCCTCCACTCGTGTCCTCTAGTCTCGCCTGGCCTCCCAG	690-HC	A8 -> TAG

Table II-1, continued

Name	Sequence	Complement	Mutation
690-HC	CTGGGAGGCCAGGCGAGACTAG AGGACACGAGTGGAGGC	689-HC	A8 -> TAG
691-HC	ATGGCTGCTTCCGCCTAGGTTGC CCGCCCTGCT	692-HC	K20 -> TAG
692-HC	AGCAGGGCGGGCAACCTAGGCG GAAGCAGCCAT	691-HC	K20 -> TAG
693-HC	AAGGTTGCCCGCCCTTAGGTCCG CGTTGCTCAGGTC	694-HC	A25 -> TAG
694-HC	GACGTGAGCAACGCGGACCTAAG GGCGGGCAACCTT	693-HC	A25 -> TAG
727-HC	GGTTCGACCATTGAACGCCATCG TCGCGGTCTCCC	728-HC	C79 -> ALA
728-HC	GGGACACGGCGACGATGGCGTTC AATGGTCGAACC	727-HC	C79 -> ALA
749-HC	CCACTCGTCTCCTCTGTTCTCGCC TGGCCTCCCAGATGG	750-HC	A8 -> CYS
750-HC	GCATCTGGGAGGCCAGGCGAGA ACAGAGGAGACGAGTGG	749-HC	A8 -> CYS
751-HC	CTCGCCTGGCCTCCCAGTGTGCT GCTTCCGCC	752-HC	M15 -> CYS
752-HC	GGCGGAAGCACCACACTGGGAG GCCAGGCGAG	751-HC	M15 -> CYS
753-HC	GTTGCCCGCCCTTGTGTCCGCGTT GCTCAG	754-HC	A25 -> CYS
754-HC	CTGAGCAACGCGGACACAAGGG CGGGCAAC	753-HC	A25 -> CYS
755-HC	GCTCAGGTCAGCAAGCGCTGTAT CCAGACTGGCTCCC	756-HC	T35 -> CYS
756-HC	GGGAGCCAGTCTGGATACAGCGC TTGCTGACCTGAGC	755-HC	T35 -> CYS
757-HC	CCCTCAAGCGCACCCAGTGTACC TCCATCGTCAACGCC	758-HC	M50 -> CYS
758-HC	GGCGTTGACGATGGAGGTACACT GGGTGCGCTTGAGGG	757-HC	M50 -> CYS
759-HC	GCCACCACCCGCTGTGCTTTCCA GAAGCGCGC	760-HC	Q60 -> CYS
760-HC	GCGCGCTTCTGGAAAGCATAGCG GGTGGTGGC	759-HC	Q60 -> CYS
761-HC	GGCTTTCCAGAAGCGCTGTTACT CTTCCGACGGCATC	762-HC	A66 -> CYS
762-HC	GATGCCGTCGGAAGAGTAACAGC CCTTCTGGAAAGCC	761-HC	A66 -> CYS
763-HC	CGCGCCTACTCTTCCTGTGGCATC ATGGTTCGTCC	764-HC	D70 -> CYS

Table II-1, continued

Name	Sequence	Complement	Mutation
764-HC	GGTCGAACCATGATGCCACAGGA AGAGTAGGCGCG	763-HC	D70 -> CYS
765-HC	GAAGAAAGACAGATCTGCCCACC ACCACCACCACCACAAGC	766-HC	C263 -> ALA
766-HC	GCTTGTGGTGGTGGTGGTGGTGG GCAGATCTGTCTTTGTTG	765-HC	C263 -> ALA
767-HC	GCCTCCACTCGTGTCTAGGCCTCT CGCCTGGCCTCC	768-HC	L7 -> TAG
768-HC	GGAGGCCAGGCGAGAGGCCTAG ACACGAGTGGAGGC	767-HC	L7 -> TAG
769-HC	CGCCTGGCCTCCCAGTAGGCTGC TTCCGCCAAG	770-HC	M15 -> TAG
770-HC	CTTGGCGGAAGAAGACTACTGGG AGGCCAGGCG	769-HC	M15 -> TAG
771-HC	GGTTGCCCGCCCTTAGGTCCGCG TTGCTCAGGTC	772-HC	A25 -> TAG
772-HC	GACCTGAGCAACGCGGACCTAAG GGCGGGCAACC	771-HC	A25 -> TAG
773-HC	CAGACCCTCAAGCGCACCCAGTA GACCTCCATCGTCAACGCC	774-HC	M50 -> TAG
774-HC	GGCGTTGACGATGGAGGTCTACT GGGTGCGCTTGAGGGTCTG	773-HC	M50 -> TAG
775-HC	GCCTCCACTCGTGTCTGCGCCTCT CGCCTGGCCTCC	776-HC	L7 -> CYS
776-HC	GGAGGCCAGGCGAGAGGCGCAG ACACGAGTGGAGGC	775-HC	L7 -> CYS
777-HC	GTTGCTCAGGTCAGCTGCCGCAC CATCCAGACTGGC	778-HC	K33 -> CYS
778-HC	GCCAGTCTGGATGGTGCGGCAGC TGACCTGAGCAAC	777-HC	K33 -> CYS
779-HC	CAGACCCTCAAGCGCACCCAGTG CACCTCCATCGTCAACGCC	780-HC	M50 -> CYS
780-HC	GGCGTTGACGATGGAGGTGCACT GGGTGCGCTTGAGGGTCTG	779-HC	M50 -> CYS
837-JS	CAGATGGCTGCTTCCGCCTGTGTT GCCCGCCCTGCTGTCCGC	838-JS	S20 -> CYS
838-JS	GCGGACAGCAGGGCGGGCAACA CAGGCGGAAGCAGCCATCTG	837-JS	S20 -> CYS
839-JS	CAGATGGCTGCTTCCGCCTAGGT TGCCCGCCCTGCTGTCCGC	840-JS	S20 -> TAG
840-JS	GCGGACAGCAGGGCGGGCAACC TAGGCGGAAGCAGCCATCTG	839-JS	S20 -> TAG
841-JS	CGCACCATCCAGACTGGCTGTCC CCTCCAGACCCTCAAGCGC	842-JS	K40 -> CYS

Table II-1, continued

Name	Sequence	Complement	Mutation
842-JS	GCGCTTGAGGGTCTGGAGGGGAC AGCCAGTCTGGATGGTGCG	841-JS	K40 -> CYS
843-JS	CGCACCATGCAGACTGGCTAGCC CCTCCAGACCCTCAAGCGC	844-JS	K40 -> TAG
844-JS	GCGCTTGAGGGTCTGGAGGGGCT AGCCAGTCTGGATGGTGCG	843-JS	K40 -> TAG

Plasmids

The plasmid pGEM 4z Su9-DHFR, containing the ORF for Su9-DHFR under control of the SP6 promoter, was a gift from Dr. Rob Jensen (Johns Hopkins University, Baltimore, Maryland). Site-directed mutagenesis of this plasmid was performed to engineer amber codons (TAG) at specific positions in the ORF. The constructs made using this technique were named Su9-DHFR TAG-X, with X indicating the number of the amino acid position containing the mutation. The positions of each of the amber mutants of Su9-DHFR are shown in Figure II-2.

Site-directed mutagenesis was also performed to engineer cysteine residues at specific positions in the Su9-DHFR ORF. The cysteine mutants were referred to as Su9-DHFR Cys-X, with the X indicating the position of the cysteine mutation, as with the TAG mutants. The positions of the Cys mutants of the Su9-DHFR constructs are also shown in Figure II-2. The native cysteine residue is located at position 79 in the construct, and was not altered.

Figure II-2. Diagram of the Su9-DHFR construct. Structure of the Su9(1-69)-DHFR construct. The yellow lines mark the positions of the TAG or Cys mutations. Only one residue position was modifed per construct.

PCR Generation of Full-length Su9-DHFR

A 5'-forward primer was synthesized that included the SP6 promoter sequence, the Kozak sequence, and the first 24 bases of the Su9-DHFR ORF (encoding the first 8 amino acids). This primer could be used for any Su9-DHFR construct to generate ssDNA for *in vitro* transcription reactions. 3'-primers were designed to generate full-length DNA products for each Su9-DHFR construct. These primers were ordered from IDT or Sigma-Genosys, and resuspended in ddH_2O to a concentration of 50 pmol/μL. The primers are listed below (Table II-2). A typical PCR reaction contained 1X ExTaq™ polymerase buffer (Takara), 200 μM each dNTP, 100 pmol each of forward and reverse primers, 100 ng template DNA, and ddH_2O to a total volume of 100μL. ExTaq™ DNA polymerase (0.5 μL,Takara) was added to each reaction, and a "touchdown" PCR reaction was performed. The PCR reaction conditions are as follows: initial heating at 94°C for 5 min, followed by 10 cycles of denaturation at 94°C for 30 sec., annealing at 70°C for 30 sec, and elongation at 72°C for 1 min, followed by 20 cycles of denaturation at 94°C for 30 sec., annealing at 57°C for 30 sec., and elongation at 72°C for 1 min. The reactions were held at 72°C for 7 min before being cooled to 4°C. At the end of the PCR reaction the PCR products were isolated using the QiaQuick PCR Purification Kit (Qiagen), and resuspended in 45 μL ddH_2O. For verification that the amplification reactions were successful, 5 μL of each sample were run on a 1% agarose gel. The other 40 μL of the PCR reaction was stored at –20°C.

Table II-2. Primers for PCR-generated DNA fragments

Name	Sequence	Template	Purpose
1058-HC	GTACATATTGTCGTTAGAACGCGGC	pGEM Su9-DHFR	upstream primer
1251-HC	GCATAGCTTTAGGAGGGGAGC	pGEM Su9-DHFR	FL Su9-DHFR
1307-HC	ATTTAGGTGACACTATAGAAACCACC ATGGCCTCCACTACTCGTGTCCTC	all Su9-DHFR constructs	upstream primer
1362-HC	GGATCTATGAACAGGAGTCCAAGC	pQE60 Su9-DHFR-Cys-	FL Su9-DHFR-Cys-His6

In vitro Transcription

A 100 μL transcription reaction contained the following: 5 μL PCR-amplified DNA (see above), 80 mM HEPES (pH 7.5), 16 mM $MgCl_2$, 2 mM spermidine, 10 mM DTT, 3 mM each ATP, CTP, and UTP, 1.5 mM GTP, 500 μM diguanosine triphosphate [G(5')ppp(5')G] (Amersham), 0.5 units pyrophosphatase, 50 units RNasin™ ribonuclease inhibitor (Promega), and 100 units of SP6 polymerase. The reactions were incubated for 90 min at 37°C, then an additional 3.2 mM GTP was added and the reaction was incubated at 37°C for another 30 min. The mRNA was typically purified using one of two methods: standard ethanol precipitation or isolation via the RNeasy® Kit (Qiagen). Regardless of the isolation method used, the samples were resuspended in 85 μL TE buffer (10 mM Tris-HCl (pH 7.5), 1 mM EDTA (pH 7.5)), and 5 μL were run on an 1.6% agarose gel for verification that the transcription was successful; the other 80 μL were stored at –80°C.

In vitro Translation

The mRNAs made in the *in vitro* transcription reactions were translated in a wheat germ cell-free translation system. A typical 25 μL reaction contained 20 mM HEPES (pH 7.5), 3 mM $Mg(OAc)_2$, 70 - 90 mM KOAc (pH 7.5), 1.6 mM DTT, 200 μM spermidine, 8 μM SAM (S-adenosylmethionine), 1X protease inhibitors, 2 μL EGS (energy-generating system with 120 mM creative phosphate, 0.12 units/μL creatine phosphokinase, and 375 μM each of the 20 amino acids), 4 μL wheat germ extract (purified according to Erickson and Blobel (year?)), 10 units RNasin™, 15 pmol [^{14}C]Lys-tRNA^{amb}, and 2 μL mRNA. For translations which would be examined by SDS-PAGE, EGS-M was used (EGS lacking methionine), and 0.2 – 1.0 μCi/μL [^{35}S]methionine (Perkin-Elmer) was added as well. Before addition of the mRNA, tRNA, and, if needed, [^{35}S]methionine, the reaction was incubated for 5 min at 26°C, to allow for unlabeled translation of any endogenous mRNAs. The reaction was placed back on ice, then the tRNA and mRNA were added, and the reaction was incubated at 26°C for another 35 min, and then returned to ice. When the translations were examined using SDS-PAGE, 2 μL of the translation reaction was added to 20 μL 1X SDS loading buffer (with DTT added) and heated to 95°C for 5 min. The samples were then loaded onto a 12.5% SDS gel and run at 100 V for 1 hour.

Import into Yeast Mitochondria

An aliquot of frozen mitochondria (0.5 – 1.0 mg) was thawed on ice (approximately 30 min.). The thawed mitochondria were resuspended in sucrose import buffer (SIB), containing 250 mM sucrose, 80 mM KCl, 5 mM $MgCl_2$, 2 mM KPO_4 (pH 7.5), 20 mM HEPES (pH 7.5), and 0.3% (w/v) BSA (Sigma A-0281), to a final concentration of 1 mg/mL. The resuspended mitochondria were then pelleted in a refrigerated centrifuge at 9000 g for 5 min at 4°C. After the supernatant was removed by aspiration, the mitochondria were resuspended in 0.2 mL SIB the amount of mitochondrial protein was determined from the A_{280} as above. Unless otherwise noted, small-scale import reactions (i.e., those used for SDS-PAGE analysis) were typically prepared using 5 μL of the translation incubation and 50 μL of 0.25 mg/mL mitochondria, along with either 2 mM each of malate and pyruvate or 2 mM each of ATP and NADH, added as ATP-regenerating substrates. The reactions were incubated at 26°C for 15 min, then placed on ice to stop the import reaction. Unless import reactions were followed with another treatment (i.e., protease digestion), the mitochondria were then centrifuged at 20,000 g and 4°C for 5 min, after which mitochondrial pellets were resuspended in SDS sample buffer (with DTT added).

Import reactions for fluorescence experiments were generally much larger, and the reaction conditions differed slightly from the smaller import reactions. Typically, 100 μL of 0.5 mg/mL mitochondria (in the presence of 2 mM malate and pyruvate) were added to 1000 μL of translation incubation, and 140 μL of 2 M sucrose was added to keep the mitochondria osmotically stable.

Occasionally, imports were performed in the absence of a $\Delta\Psi$, which would prevent the precursor protein from crossing the IM. Under these conditions, 50 μM carbonyl cyanide 3-chlorophenylhydrazone (CCCP, Sigma C-2759) was added to the import reactions to dissipate the membrane potential across the IM before the import reactions were completed as above.

Generation of Mitochondrial Import Intermediates

To generate an import intermediate across both mitochondrial membranes, methotrexate (MTX; Sigma M-9929), a substrate analog for DHFR, was added to the samples after the translation reaction. Addition of methotrexate to Su9-DHFR causes the DHFR domain to fold tightly, preventing it from being pulled across the mitochondrial membranes. In this way, an import intermediate can be created in which the Su9 presequence crosses both the OM and IM and is bound in the matrix by mtHsp70, while the DHFR polypeptide remains on the cytosolic side of the OM. A 10 mM MTX stock was made by diluting 4.5 mg of MTX into 50 μL of 3 N NaOH. The volume was then brought up to 1 mL with SIB, and the stock was stored in at –20°C. For each experiment, the 10 mM stock was thawed and diluted 1:100 in SIB to make a 100 μM MTX solution. To generate Su9-DHFR•MTX intermediates, MTX was added to a final concentration of 2 μM at the end of a translation reaction and the samples were allowed to incubate on ice for 5 min. Mitochondria were then added to the reactions as described above, except that a concentration of 2 μM MTX was kept in the import reactions, to avoid diluting the MTX and losing the import intermediates.

Preparation of Fluorescent Samples

To perform collisional quenching experiments, mitochondrial import intermediates were generated using the conditions described above, except that each experiment required two reactions, one in the presence of εNBD-[^{14}C]Lys-tRNA^{amb} (termed the Sample) and the other in the presence of unmodified [^{14}C]Lys-tRNA^{amb} (the Blank). After completion of the import reaction, the mitochondria were pelleted for 5 min at 10,000g, in a refrigerated centrifuge, and the supernatant was then aspirated. The mitochondria were resuspended in 1 mL of Buffer A/K^+/E (similar to the SLM Buffer, except for the presence of 250 mM KOAc (pH 7.5) and 60 mM EDTA) and allowed to incubate on ice for 15 min. The mitochondria were then pelleted again for 5 min at 10,000g and 4°C, the supernatant was aspirated, and the sample tubes were then pulsed again (at 10,000g, about 30 sec) to ensure that all liquid in the tubes had sedimented to the bottom. This liquid was also removed, and the mitochondria were resuspended in 350 μL of SLM Buffer. When the samples being analyzed were import intermediates, 2 μM MTX was kept in the buffers at all times.

Fluorescence Spectroscopy

All fluorescence experiments were performed in an SLM Aminco 8100 photon-counting specrofluorimeter using 4 mm x 4 mm square quartz microcell cuvettes (Starna) and a temperature of 4°C. The cuvette chamber was continuously flushed with N_2 to prevent condensation of water on the cuvettes. Each cuvette had a small magnetic "stir flea" at the bottom to mix samples after each addition as described (Dell et al, 1990)

and the cuvettes were always re-equilibrated to 4°C before any readings were taken. To eliminate light scattering and background signal from the observed NBD fluorescence intensity of the Sample, both the Sample and Blank intensities were measured using excitation and emission wavelengths of 468 nm and 485 nm, respectively, with a 4 nm bandpass. The Sample and Blank were equalized with respect to the amount of background and scattering signal by diluting the sample with the higher signal until both the Sample and Blank had the same emission intensity at 485 nm. The emission was then scanned at 1 nm intervals between 490 and 600 nm. Emission spectra were taken of both the Sample, containing NBD, and the Blank, lacking NBD, and the spectrum of the Blank was subtracted from the Sample spectrum to obtain the net NBD emission spectrum.

Collisional Quenching of NBD with Iodide Ions

Aliquots (150 uL) of the Sample, containing NBD, and of the Blank, lacking NBD, were distributed to two microcells each, termed S1 and S2 and B1 and B2. The fluorescence intensities of all cuvettes were read using excitation and emission wavelengths of 468 nm (bandpass = 4 nm) and 530 nm (bandpass = 4 nm), respectively, and the initial net NBD fluorescence (F_0) was calculated by subtracting the Blank signal from the Sample signal (B1 from S1, and B2 from S2). Then iodide ions (5 μL of 0.8 M KI) were added to S1 and B1, and the net fluorescence intensity was measured again. As a control for any effects of increasing ionic strength on the sample NBD intensities, 5 μL of 0.8 M KCl were added to S2 and B2 and the net fluorescence intensity was

determined. The KCl and KI additions were repeated two more times, so that emission intensities (F) were measured at KI or KCl concentrations of 0, 25, 50 or 72 mM. Corrections were made to each intensity reading to account for dilution effects. Alamethicin (ALA) was then added each cuvette as described above, and the fluorescence intensities were measured again.

For steady-state collisional quenching of fluorescence, the data were analyzed according to the Stern-Volmer law:

$$(F_0/F) - 1 = K_{sv}\,[Q] \quad (2)$$

where K_{sv} is the Stern-Volmer quenching constant and Q is the concentration of quencher. There was minimal decrease in NBD emission intensity at increasing KCl concentrations, revealing that NBD fluorescence and sample constituents were minimally affected by increasing ionic strength. The iodide K_{sv} was then determined by first using non-linear regression to ascertain the slope of the "best-fit" straight line through the KI data. This analysis was repeated for the KCl data to determine the chloride K_{sv}. The net iodide K_{sv} was then determined by subtracting the best-fit KCl K_{sv} from the best fit KI K_{sv} (Crowley et al, 1993). A typical experiment is shown in Figure II-3.

Biochemical Analysis of Fluorescent Samples

At the conclusion of each fluorescence experiment, the volume from each cuvette was collected and the radioactivity (hence, NBD probe) content was determined using a liquid scintillation counter. Typically, sample volume was adjusted to a final volume of

400 μL and put into a 5 mL insert vial, 4 mL of Trition-based scintillation cocktail was added, and the ^{14}C cpm (counts per minute) were measured. Alternatively, half of the volume (~80 μL) was added to an insert vial to determine the total Triton ^{14}C counts, while the mitochondria in the other half of the sample were sedimented for 10 min, 20,000g and 4°C in a microfuge. The supernatant was removed, put into an insert vial and counted as above, while the mitochondrial pellet was resuspended in 400 μL of 2% (w/v) SDS before being transferred to an insert vial and determining the ^{14}C cpm as above. By splitting the volume of the fluorescent samples, it was possible to determine the total cpm of the sample as well as the cpm that remained associated with the mitochondria. The ratio of the net NBD emission intensity in pulses per second (pps) to the number of NBD probes in the sample in cpm was determined for each fluorescence experiment. Any change in the pps/cpm ratio for a particular construct would indicate that the environments of some or all of the NBD dyes had changed.

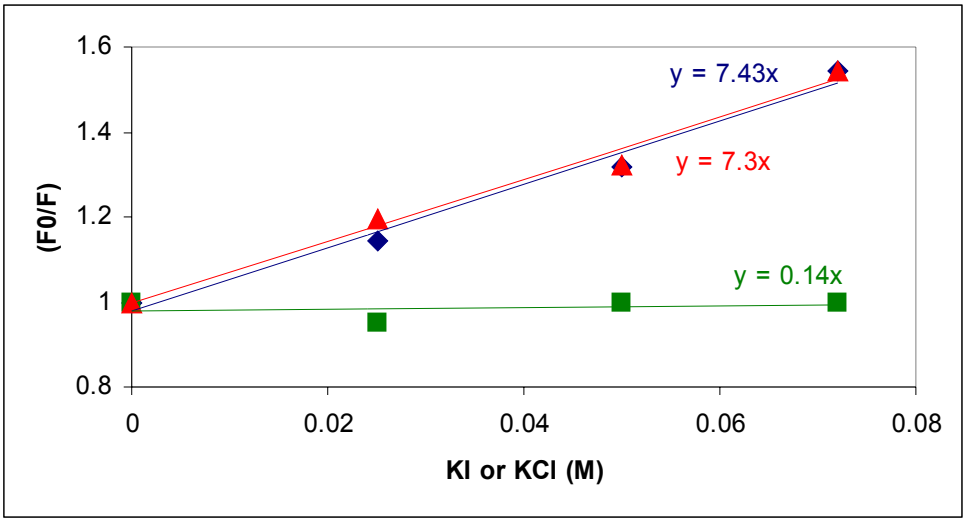

Figure II-3. Stern-Volmer plot for collisional quenching of NBD-Su9-DHFR by KI. After import of NBD-Su9-DHFR presequences, in the presence of absence of MTX, the Sample (containing NBD) and the Blank (lacking NBD) are titrated with both KI and KCl. The titration data for KI is shown in blue, and the titration data for KCl is shown in green. The net F_0/F, obtained by subtraction of the KCl data from the KI data, is shown in red. The slope of each regression line (Stern-Volmer quenching constant, or K_{sv}) is shown in the identical color.

Protease Digestions

After completion of import reactions, the samples were split into two aliquots (one for protease digestion, one for a negative control). To the aliquot that would receive the protease treatment, 1 mg/mL proteinase K (Sigma P-2308) was added to a concentration of either 50 μg/mL ("light" protease digestion) or 100 μg/mL ("typical" protease digestion). Occasionally, 50 μg/mL trypsin (Sigma, T-8642) was added to the import reactions instead. The samples were allowed to incubate on ice for 15 min, then the reactions were quenched with either 1 mM PMSF (Sigma, P-7626) for the proteinase K reactions or 100 μg of trypsin inhibitor (Sigma, T-9003). The reactions were centrifuged at 20,000 g for 5 min at 4°C in a microcentrifuge. The supernatants were aspirated and the mitochondrial pellets resuspended in SDS Sample Buffer (+DTT) before being analyzed by SDS-PAGE.

Alamethicin Treatments

To perforate the mitochondrial IM, the pore-forming antibiotic alamethicin (ALA; Sigma A-4665) was added to a final concentration of 3.5 – 8 ug/mL, and the samples were allowed to incubate at room temperature for 10 min.

Propidium Iodide Assay of Mitochondrial IM Integrity

In order to assay the integrity of the IM of the isolated mitochondria, advantage was taken of the fact that mitochondria possess their own genomic DNA, located in the mitochondrial matrix. By adding a DNA-intercalating fluorescent dye to the

mitochondria, the integrity of the IM could be evaluated by comparing the fluorescence intensity of the dye before and after the addition of alamethicin, an antibiotic that forms holes in the mitochondrial IM. To perform this experiment, mitochondria were washed in SIB and centrifuged as above, but were then resuspended in PI Buffer (20 mM HEPES (pH 7.4), 3 mM $Mg(OAc)_2$, 70 mM KOAc (pH 7.4), 250 mM sucrose). After an A_{280} reading of the mitochondria was taken as described previously to calculate the amount of mitochondrial protein, the mitochondria were resuspended to a concentration of 0.25 mg/mL and 250 μL were then added to a quartz microcell (250 μL PI Buffer was added to another microcell for blank subtraction). A working solution of 100 μM propidium iodide (Molecular Probes, P-3566) was made by diluting the 1.5 mM stock into H_2O. The fluorescence intensities of the sample and blank were read at an excitation wavelength of 535 nm and an emission wavelength of 617 nm, with the temperature of the fluorimeter turret kept at 4°C. Propidium iodide (5 μL of 100 μM) was added to both microcells and the intensities were read again. ALA (5 μL of 5 mg/mL) was then added to both microcells and the samples were allowed to incubate at room temperature for 10 min. After the microcells were returned to the fluorimeter turret and allowed to equilibrate to 4°C, the fluorescence intensities were read again. The readings were corrected to adjust for dilution, and the fluorescence intensities before and after addition of ALA were then compared by reporting the –ALA intensity of a sample as a percentage of it's +ALA reading. This percentage was then taken to be equal to the fraction of mitochondria whose IM was no longer intact and sealed.

JC-1 Assay of Mitochondrial Membrane Potential

The membrane potential of the mitochondrial inner membrane was monitored using the potentiometric dye JC-1. JC-1 (Molecular Probles, T-3168) partitions into the mitochondrial IM and exists as a monomer when the potential difference across the membrane is low. But in the presence of higher potentials, JC-1 will form "J-aggregates". The fluorescence excitation and emission maxima are distinctly different under these two conditions, making it possible to monitor the potential of the mitochondria by comparing the fluorescence intensities of the monomer peak and the J-aggregates peak. Typically, mitochondria were thawed and washed as described above, then resuspended to a concentration of 12.5 ng/mL in SLM Buffer (20 mM HEPES (pH 7.5), 3 mM $Mg(OAc)_2$, 25 mM KOAc (pH 7.5), 250 mM sucrose, 2 mM malate, 2 mM pyruvate). The JC-1 dye was resuspended in DMSO to a stock concentration of 1.5 mM and was kept at –20° C. For each experiment, the stock was diluted to 150 nM in DMSO. To perform the fluorescence experiments, bandpass on the SLM fluorimeter was set to 1 nm, and the excitation and emission monochromators were set to 575 nm and 590 nm, respectively. For a time trace, 3.5 μL of 150 nM JC-1 were added to 250 μL mitochondria in a quartz microcell, and the fluorescence intensity monitored over 1200 sec. About 120 sec before the end of the scan 50 mM CCCP was added to depolarize the mitochondria inner membrane, to verify that the fluorescence intensity being monitored was due to the mitochondrial membrane potential. For emission scans, the excitation monochromator was set to 485 nm and the emission monochromator was scanned from 500 – 600 nm. The intensities of the monomer peak (540 nm) and

aggregate peak (590 nm) were then compared to gauge the extent of membrane polarization.

Chemical Crosslinking

Chemical crosslinking reactions were performed using mitochondrial import intermediates to analyze the positions of the intermediates relative to the import machinery. The reagent BMH (Pierce, 22330) is a homobifunctional cysteine-cysteine crosslinker with a spacer arm of 16 Å that can be used in conjunction with the Su9-DHFR Cys mutants. Import intermediates were made using the Su9-DHFR Cys constructs and MTX, as described previously. After the import reaction, BMH was added to a final concentration of 100 μM and the samples were incubated at room temperature for 35 min (control reactions were performed in the presence of DMSO, the BMH solvent). The samples were then quenched by the addition of 70 mM Tris-HCl (pH 7.5), and 70 mM DTT, and incubation at room temperature for another 15 min. The mitochondria were then sedimented and the samples prepared for SDS-PAGE as described above.

CHAPTER III

RESULTS

Necessity for Developing a Fluorescence-based System

The field of mitochondrial protein import has made many advances in the past two decades, much of which is summarized in Chapter I. Previously, it had been believed that proteins destined for the mitochondria spontaneously crossed the outer and inner membranes (OM and IM), without the aid of transport systems. However, over the past twenty years more than 25 proteins, in more than six separate translocons, have been discovered occupying both the OM and IM, as well as residing in the IMS and matrix, to aid protein translocation across the mitochondrial membranes. Most of the Tom and Tim proteins were discovered using either yeast genetic techniques or *in vitro* binding studies, or by examining open reading frames (ORFs) from the yeast genome database. However, in order to understand more fully the operation of the mitochondrial protein import pathways, it would be useful to examine these pathways from the perspective of a translocating polypeptide. By site-specifically positioning a fluorescent probe into a matrix-targeted protein it becomes possible to take advantage of the properties of the probe, such as accessibility to an externally added quencher or changes in the fluorescent lifetime of the probe in response to the probe's environment.

Site-specific fluorescence and photocrosslinking experiments of the kind proposed for this project have been used to examine protein translocation across, and integration into, the endoplasmic reticulum (ER) membrane. Briefly, the environmentally sensitive fluorophore NBD was site-specifically incorporated into the

secretory protein preprolactin (pPL) by adding NBD-labeled lysine tRNAs to the translation reaction (Crowley et al, 1994). In the presence of isolated ER microsomes, the resulting NBD-labeled ribosome-nascent chains (RNCs) formed translocation intermediates at the ER translocon, with the position of the NBD probe along the translocation channel dictated by the location of the probe in the nascent chain and the length of the truncated mRNA used in the translation reaction. By monitoring the fluorescent lifetime of the NBD probe under these experimental conditions, the authors were able to determine that the nascent chain moves through an aqueous tunnel as it crosses the ER membrane (Crowley et al, 1994).

Subsequent work by Hamman et al, (1997) employed collisional quenching of the fluorescent-labeled, membrane-bound RNCs with externally added (thus, cystoplasmic) iodide ions. The authors found that as the NBD probe moved through the ribosomal tunnel and the translocon it was inaccessible to these cytoplasmic iodide ions, indicating that the ribosome forms a tight seal with the translocon on the cytosolic side of the membrane, sealing off the nascent chain from the cytoplasm and preventing ion leakage from the ER lumen through the translocon during translocation. Immediately after targeting, the nascent chain was also inaccessible to quencher in the ER lumen (Crowley et al, 1999) because BiP closed the lumenal end of the aqueous pore either directly or indirectly (Hamman et al, 1998). However, when the length of the nascent chain was increased to longer than 70 residues, the fluorescent probes located inside the ribosome become accessible to collisional quenching from the lumenal side of the ER membrane (Crowley et al, 1994; Hamman et al, 1997). Indeed, quenchers as large as

NAD^+ were able to quench the NBD probes located in the ribosome tunnel of the membrane-bound RNCs, which suggested that the pore of an active translocon is as large as 60 Å in diameter (Hamman et al, 1997).

These data then raised the question of what protein or complex maintains the permeability barrier of the translocon in the absence of a translating ribosome. Collisional quenching experiments on ER membranes showed that a ribosome-free translocon has a pore size of 10-15 Å, much smaller than that of an active translocon, and that the luminal protein BiP maintains the permeability barrier from the luminal side of the translocon (Hamman et al, 1997, 1998).

Fluorescence spectroscopy proved supremely useful in studying ER translocation because this approach allowed the translocation pathway to be studied from the perspective of the nascent chain in a functional system. Many of the questions answered in the ER system are pertinent to the field of mitochondrial protein import: Does a translocating preprotein cross the IM via an aqueous channel? How is the IM membrane potential maintained during translocation through the TIM23 complex? Is a translocating preprotein ever exposed to the IMS during translocation through the TOM and TIM23 complexes? The goal of this project was to apply spectroscopic techniques to study translocation through the mitochondrial import system in order to address some of the questions that could not be answered using conventional cell biology techniques. These techniques included site-specifically labeling a model matrix protein with a fluorescent dye, generating import intermediates with the labeled matrix protein, and analyzing the fluorescent properties of the dye in the resultant complexes.

Experimental Design

The model matrix protein Su9(1-69)-DHFR has been used in previous mitochondrial import experiments to generate translocation intermediates. It consists of the matrix-targeted presequence of subunit 9 of the F1-Fo ATPase, fused to dihydrofolate reductase (DHFR) as the passenger protein. The Su9 presequence is sufficient to direct the protein to isolated mitochondrial (Hurt et al, 1994), and, in the presence of the folate analog methotrexate (MTX), the DHFR moiety will fold into a tight complex (Eilers and Schatz, 1986). In the presence of mitochondria and an ATP-regenerating system the polypeptide will be imported until the tightly folded DHFR•MTX complex reaches the OM, generating a stable import intermediate with the DHFR domain on the outside of the mitochondria. The Su9 domain spans both the OM and IM, and is held in place by the binding of mtHsp70 to the presequence residues exposed to the mitochondrial matrix. This system has been used previously to study the mitochondrial import pathway (Pfanner et al, 1987b; Vestweber et al, 1989; Ryan and Jensen, 1993). However, by incorporating fluorescent dyes site-specifically into the Su9-DHFR construct, we will be able to examine the environment surrounding the modified residue as it is being imported.

Previous work in the Johnson lab has used modified lysine tRNAs to site-specifically incorporate a fluorescent or photoreactive probe into the protein of interest. This approach would, in principle, place a modified lysine into any position denoted with a lysine codon. But since the Su9-DHFR construct has 20 lysines, another method was required to allow incorporate only a single modified residue in each polypeptide.

The Johnson Lab had developed a system whereby amber suppressor tRNAs were charged with lysine, and the resultant Lys-tRNA^{amb} were modified with the NBD moiety, generating εNBD-Lys-tRNA^{amb} (Flanagan et al, 2003). Site-directed mutagenesis could then be used to mutate the desired codon of an ORF to an amber codon, and translation of mRNAs transcribed from the mutated DNA construct would allow for incorporation of a modified residue only at the position of the amber codon. Another advantage of the suppressor tRNA system was that any full-length proteins generated would necessarily contain the probe on the modified lysine, because the only competition for the modified Lys-tRNA^{amb} would come from endogenous termination factors that would release the nascent chain from the peptidyl-tRNA and thereby halt translation. These prematurely terminated nascent chains would not have a fluorescent probe, so they would be invisible in the fluorimeter. Hence, site-directed mutagenesis was performed on the Su9-DHFR construct to replace the codons for residues 8, 15, 20, 25, 33, 40, 50, 60, 66, or 70 with an amber codon (one mutated position in each construct). These constructs will hereafter be referred to as Su9-DHFR TAGX, where X is the number of residue mutated to an amber codon.

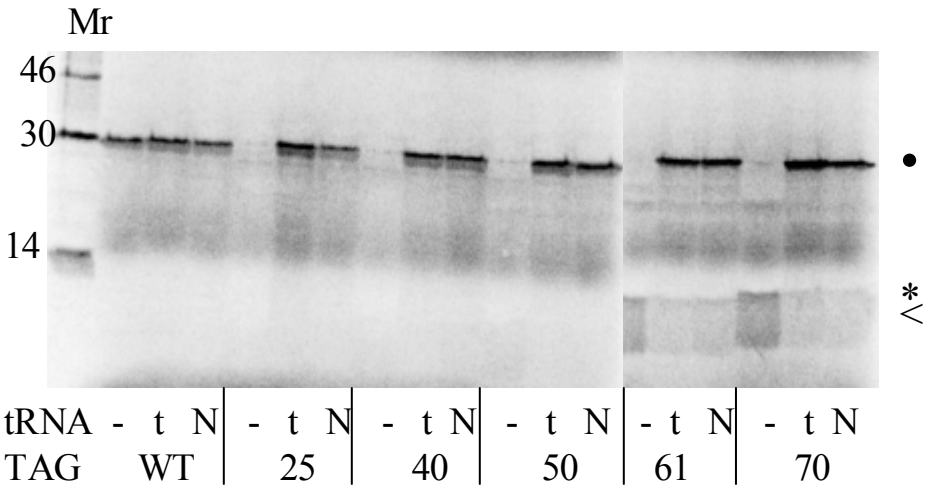

Figure III-1. Translation of Su9-DHFR TAG mutants. Su9-DHFR TAG mutants were translated as described in Experimental Methods, in the presence of either [^{14}C]Lys-tRNA^{amb} (t), or εNBD-[^{14}C]Lys-tRNA^{amb} (N). The position of each TAG is denoted on the figure. The full-length Su9-DHFR polypeptide is indicated by the closed circle (•). With the exception of the TAG61 (<) and TAG70 (*) constructs, the prematurely-terminated polypeptides are too small to be seen on the on the gel.

Incorporation of NBD into Su9-DHFR TAG Mutants

Labeling of the Su9-DHFR TAG mutants with the NBD probe relied on incorporation of the probe into the TAG position. Figure III-1 shows some of the Su9-DHFR TAG mutants translated in the presence of either unmodified [^{14}C]Lys-tRNA^{amb} or εNBD-[^{14}C]Lys-tRNA^{amb}. While the WT construct is translated even in the absence of the suppressor tRNAs, the TAG mutants are only translated in the presence of suppressor tRNA. In addition, the presence of the NBD does not inhibit lysine incorporation.

One other effect to be considered would be inhibition of import by the size of the fluorescent probe. Previous work by Schwartz and Matouschek (1999) attempted to address the pore size of the TIM23 complex by importing matrix-targeted proteins labeled with gold particles of either 20 or 26 Å. The precursor proteins with the 20 Å gold particles could be imported across the IM, while the precursor proteins labeled with the 26 Å gold particle were not. The fluorescent dye NBD attached to the ε-carbon of the lysine side chain has a diameter much less than 20 Å, so import of NBD-Su9-DHFR polypeptides was not expected to be diminished, relative to unlabeled Su9-DHFR. When import of NBD-Su9-DHFR was tested by importing a radiolabeled Su9-DHFR TAG mutant that was translated in the presence and absence of εNBD-[^{14}C]Lys-tRNA^{amb} and analyzing import efficiency via SDS-PAGE and autoradiography (Figure III-2), the presence of the NBD probe in the Su9-DHFR presequence only slightly inhibited import efficiency. Hence, one can successfully generate import intermediates with the fluorescent-labeled Su9-DHFR constructs.

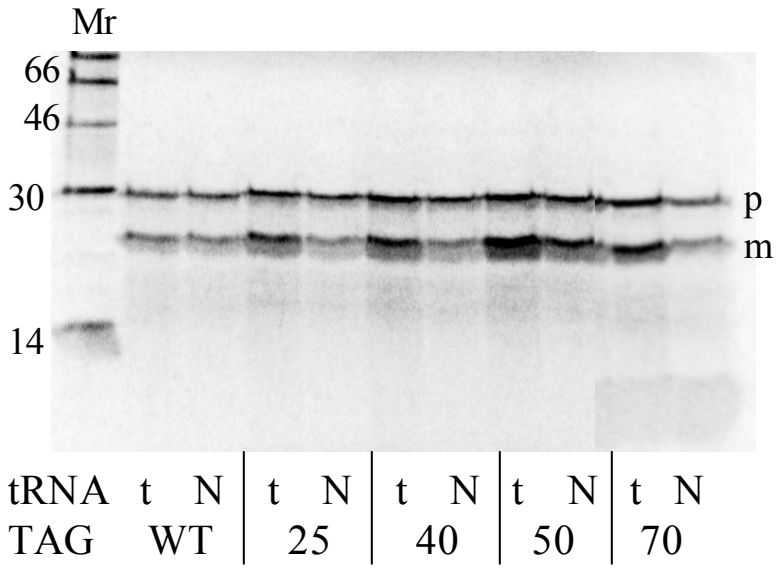

Figure III-2. Su9-DHFR TAG mutants are imported in the presence of the NBD probe. Su9-DHFR TAG mutants were translated and imported as described in Experimental Methods, in the presence of either [^{14}C]Lys-tRNA^{amb} (t), or εNBD-[^{14}C]Lys-tRNA^{amb} (N).

Generation of Mitochondrial Import Intermediates

Two methods for generating mitochondrial import intermediates are the use of DHFR•MTX, as has been done previously in the mitochondrial field, or the import of NBD-labeled nascent chains that are still bound to ribosomes to form ribosome•nascent chain complexes (RNCs), as has been done previously in the Johnson lab. While the use of DHFR•MTX intermediates is the traditional method, generating import intermediates using RNCs, if successful, would have some important advantages. This approach would require mutating only one position in the Su9-DHFR construct to an amber codon. PCR would then be performed on the ORF to make DNA fragments of different lengths. Transcription of these DNA fragments would generate truncated mRNAs (i.e., mRNAs lacking a stop codon). Translation of these truncated mRNAs, results in the formation of RNCs because the ribosome will half at the end of the truncated mRNA. Since there is no stop codon, the nascent chain remains attached to the tRNA, and one creates an RNC sample in which all of the nascent chains have the same length (Crowley et al, 1994). When these RNCs were added to a mitochondrial import reaction, the nascent chains would presumably be imported until the ribosome reached the TOM complex and halted further import. As long as the nascent chain was long enough to cross both membranes and interact with mtHsp70 (~55 residues, Ungermann et al, 1994) a stable import intermediate would be generated. By varying the length of nascent chain used in the reaction, one could position the single probe at different locations along the import pathway. In the end, this approach was abandoned because of high fluorescence

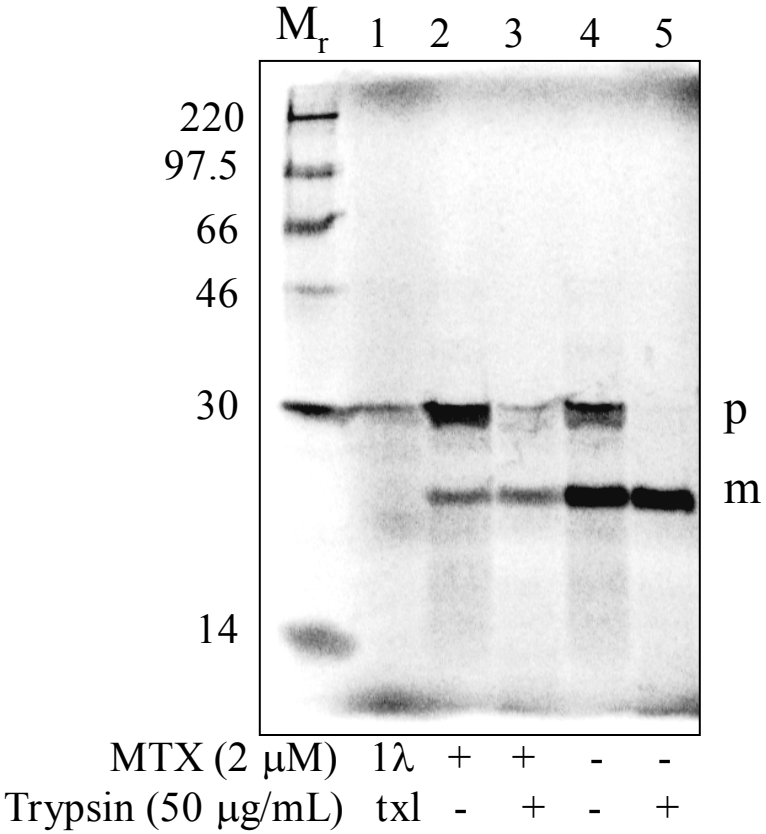

Figure III-3. Imports of Su9-DHFR into mitochondria in the presence and absence of methotrexate. Radiolabeled Su9-DHFR TAG15 was imported into mitochondria in the presence or absence of MTX, as described in Experimental Procedures. After import, the samples were split and either treated with 50 μg/mL trypsin or left untreated. p, precursor; m, mature. Lane 1 (1λ txl) refers to 1λ of the translation reaction, before addition of mitochondria.

background signals, apparently due to NBD binding to the ribosome (Kenner and Aboderin, 1971), and despite many attempts to reduce this background.

Therefore, it was decided to generate import intermediates using MTX binding to the DHFR domain. Full-length Su9-DHFR TAG mutants were translated and then imported into mitochondria in the presence of 2 μM MTX. The position of the NBD probe along the import pathway was therefore dictated by the location of the mutated residue in the polypeptide. Because the Su9-DHFR•MTX complex can only be imported until the DHFR domain reaches the OM, the matrix processing protease (MPP) processing sites of the Su9 presequence (residues 33 and 66) do not reach the matrix-side of the IM. The extent of DHFR•MTX import intermediate formation can therefore be assayed by comparing the relative amounts of the mature and processed protein on an SDS gel (Figure III-3). Any mature (processed) protein has to have been translocated into the matrix, and hence could not have been anchored by a folded DHFR domain at the TOM Complex. But any protease-sensitive precursor (full-length) Su9-DHFR would have to have been trapped at the TOM complex by a folded DHFR•MTX domain. To maximize and stabilize the formation of the tightly-folded DHFR conformation, MTX was used in all buffers subsequent to the import reaction.

Preparation of Import Samples for the Fluorimeter

To evaluate an *in vitro* import reaction using fluorescence spectroscopy, the published import protocols had to be made changed. For example, all necessary buffers and reagents had to be monitored for any contaminating materials that would scatter

light or emit fluorescent light at the wavelengths being monitored. For this reason, sucrose was used instead of sorbitol to make the import reactions osmotically stable to the mitochondrial, because the sorbitol used for isolation of the mitochondria had too many fluorescent contaminants. Malate and pyruvate were also chosen for the ATP-regenerating system, instead of ATP and NADH, because NADH has been shown to quench NBD fluorescence (Hamman et al, 1997); thus, any extra NADH would decrease the signal intensity via collisonal quenching of the NBD probes. Import reactions performed in the presence of 2 mM malate/pyruvate were as efficient as those performed in the presence of ATP/NADH (Fig III-4, compare lanes 1 and 6). Finally, the amount of mitochondria in the import reactions was significantly lowered for the fluorescence experiments. Mitochondria have significant autofluorescence, likely due to the electron transport complexes in the IM, and large amounts of mitochondria in the sample cuvettes resulted in inner filter effects and a decreased signal to noise ratio. As shown in Figure III-5, decreasing the concentration of mitochondria in the import experiments from 1.0 mg/mL (typical *in vitro* import conditions) to 0.02 mg/mL did not decrease the amount of imported preprotein because the amount of available TOM and TIM23 complexes were still not limiting.

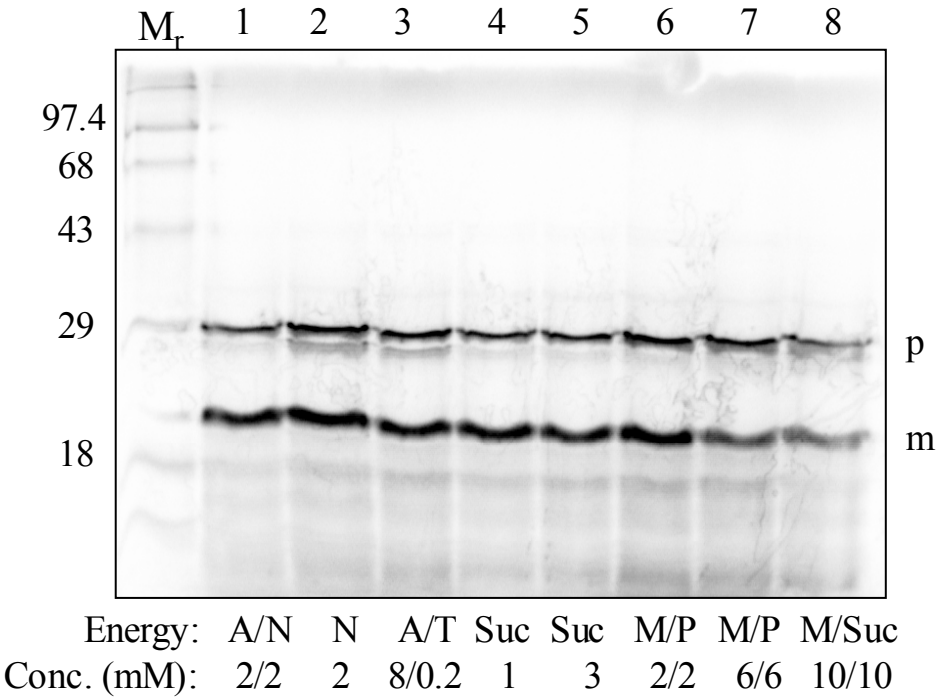

Figure III-4. Mitochondrial imports using different ATP-regenerating systems. Radiolabeled Su9-DHFR was imported into isolated mitochondria in the presence of ATP/NADH (A/N); NADH alone (N); ATP/TMPD (A/T); succinate (Suc); malate/pyruavte (M/P); or malate/succinate (M/Suc). The concentrations used are listed below. p, precursor; m, mature bands.

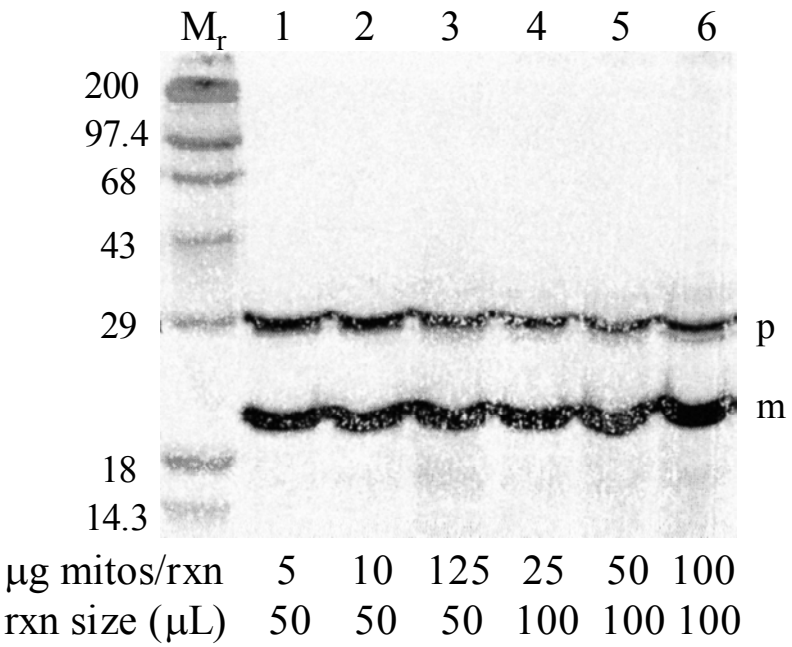

Figure III-5. Su9-DHFR imports into mitochondria using different amounts of membranes. Su9-DHFR was translated, then the reaction was split and equal amounts of precursor protein were put into import reactions containing different amounts of mitochondria. p, Su9-DHFR precursor; m, mature protein.

Once the import reactions had gone to completion, the import intermediates were purified from the rest of the reaction. Traditionally, ER microsomes were purified away from the rest of the translation reaction using size-exclusion column chromatography. But the yeast mitochondria membranes could not be isolated using this same technique because a significant percentage of the mitochondria remained at the top of the column, probably because they were too large to enter the resin. This reduced the yield of purified import intermediates, and hence the fluorescence signal of the purified sample. However, my attempts to use size-exclusion chromatography to isolate mitochondrial import intermediates did reveal the necessity of keeping an ATP-regenerating system in the mitochondrial buffers at all times. Mitochondria isolated over a Sepharose CL-2B column (Sigma) were analyzed in the fluorimeter using the potentiometric dye JC-1. When the column buffer contained 2 mM malate, 2 mM pyruvate, and 2 mM KPO_4 (pH 7.4), the mitochondria maintained their membrane potential ($\Delta\Psi$) during the chromatography (Figure III-6, green triangles). However, in the absence of this ATP-regenerating system, the mitochondria became depolarized during chromatography (Figure III-6, blue diamonds). A mitochondrial sample kept in a buffer lacking the malate, pyruvate, and KPO_4, but not isolated using chromatography, was not depolarized (Figure III-6, red squares). But the lower J-aggregate peak, compared to the mitochondria kept in the ATP-regenerating buffer, indicates a lowered membrane potential. This was an important finding because maintenance of the population of import intermediates requires a stable membrane potential across the IM.

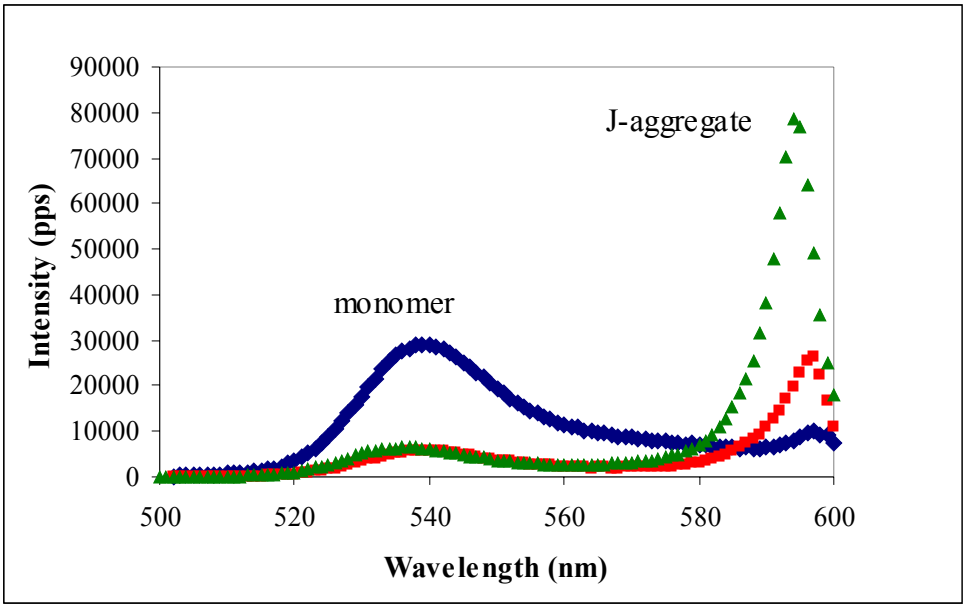

Figure III-6. Emission scans of JC-1 fluorescence in the presence of mitochondria before/after column chromatography. Mitochondria were collected before and after isolation with a CL-2B column, and then incubated with 1 ng/µL JC-1 as described in Experimental Procedures. Emission scans were taken at an excitation wavelength of 485 nm. Red squares, before column; blue diamonds, after column; green triangles, after column, in the presence of 2 µM each malate, pyruvate, and KPO_4. The monomer and J-aggregate peaks are indicated.

The loss of the $\Delta\Psi$ allows the partially imported Su9-DHFR polypeptide to diffuse out of the mitochondrial IM and OM and back into the cytosol.

In the end, the import intermediates were isolated via sedimentation rather than size exclusion chromatography. The mitochondria were sedimented at speeds of about 10,000g in a refrigerated centrifuge for 5 minutes. This allowed the mitochondria to collect at the bottom of a microfuge tube in a loose pellet that could be easily resuspended into the SLM buffer. After the first centrifugation step, the supernantant was aspirated and the mitochondria were washed in an SLM buffer containing 250 mM KOAc (pH 7.4) and 60 mM EDTA to release any adsorbed tRNA or preprotein from the OM. The mitochondria were centrifuged again and resuspended in the final SLM buffer. Each resuspension buffer contained 2 mM malate, 2 mM pyruvate, 2 mM KPO_4 (pH 7.4) and 2 μM MTX at all times.

Characterization of Imported NBD-Su9-DHFR

Before any fluorescence data on the mitochondrial import intermediates could be collected and analyzed, certain experiments were necessary to characterize the state of the import intermediates in the fluorimeter. As mentioned earlier, the isolated mitochondria and buffer components needed to be evaluated in the fluorimeter (SLM) for any background fluorescence or light-scattering material. As seen in Figure III-7, the SLM Buffer, containing HEPES and sucrose, did not fluoresce significantly at the emission wavelength of 485 nm and the excitation wavelength of 530 nm. The Import Buffer, containing both sorbitol and BSA, had a higher signal in the fluorimeter. The

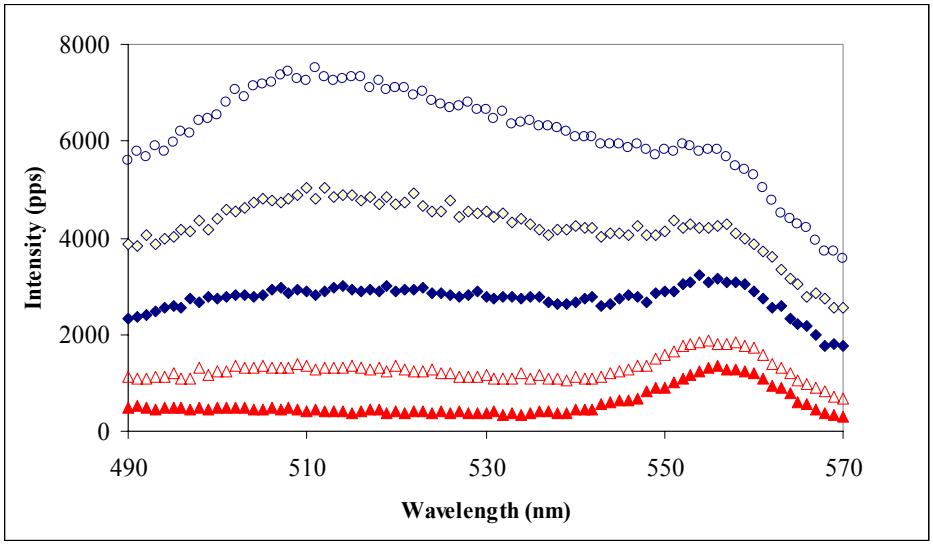

Figure III-7. Emission scans of mitochondria and buffers. Emission scans of isolated mitochondria or buffers alone at the excitation wavelength of 468 nm. ▲ , SLM Buffer; △, 0.05 mg/mL mitos in SLM Buffer; ◆ Import Buffer; ◇, 0.05 mg/mL mitos in Import Buffer;○ , 0.1 mg/mL mitos in Import Buffer.

mitochondria themselves had significant fluorescence intensity at these wavelengths, but since both the sample, containing the NBD-labeled Su9-DHFR, and the blank, containing the unlabeled preprotein, would have the same concentration of mitochondria, this background fluorescence could be subtracted from the sample fluorescence to obtain the net NBD emission. The typical concentration of mitochondria in the cuvettes was around 0.15 mg/mL.

To determine the net NBD signal for the imported Su9-DHFR, two samples were prepared in parallel. One, termed the Sample, contained the εNBD-[^{14}C]Lys-tRNA^{amb} in the translation reaction, and the other, termed the Blank, contained unmodified [^{14}C]Lys tRNA^{amb}. The Sample and Blank would then be spectroscopically identical except for the presence of the NBD fluorophore. After the translation, import, and isolation of the import intermediates, the Sample and the Blank were normalized with respect to the amount of light scattering material as described in Chapter II. Fluorescence emission scans of the both the Sample and Blank were taken using an excitation wavelength of 485 nm and scanning the emission from 490 – 600 nm. By subtracting the emission scan of the blank from that of the sample the net NBD emission scan was obtained.

To ensure that any NBD fluorescence observed was due to the presence of NBD in Su9-DHFR and not unincorporated εNBD-[^{14}C]Lys-tRNA^{amb}, emission scans were taken from mitochondria isolated from translation and import reactions performed in the presence and in the absence of Su9-DHFR mRNA. As can be seen in Figure III-8, the NBD signal of mitochondria containing imported NBD-Su9-DHFR TAG50 or TAG75 was around 2000 and 3500 pulses per second (pps), respectively. The NBD signal from

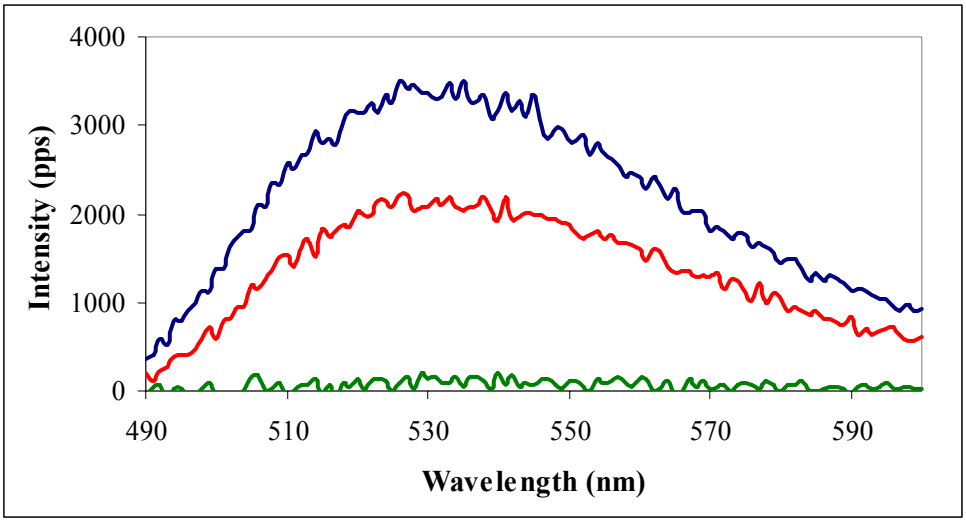

Figure III-8. The NBD fluorescence of imported Su9-DHFR is due to incorporation of NBD into nascent chains. Su9-DHFR TAG50 (red), and TAG70 (blue) were translated in the presence of εNBD-[^{14}C]Lys-tRNA^{amb} and imported into isolated mitochondria as described in Experimental Methods. NBD emission scans were recorded using an excitation wavelength of 468 nm. An identical reaction, performed in the absence of any Su9-DHFR mRNA, showed no NBD fluorescence (green). The spectra shown are the net NBD signals obtained after subtraction of the background signals of parallel samples lacking NBD.

the mitochondria isolated from the translation/import reaction that lacked mRNA had negligible fluorescence, indicating that the NBD signal observed in the fluorimeter was indeed due to the presence of the NBD incorporated into Su9-DHFR. Differences in the fluorescence intensities of the different TAG mutants was likely due to the difference in the suppression efficiencies at each TAG position.

The fluorescence signal of imported NBD-Su9-DHFR was observed as a function of time in the fluorimeter to detect whether any sedimentation of the mitochondria occurred during the course of a fluorescence experiment. Mitochondria containing imported NBD-Su9-DHFR TAG25 were monitored using excitation and emission wavelengths of 468 nm and 530 nm, respectively, over the course of 60 minutes. Any significant sedimentation of the mitochondria would result in the membranes sinking below the light path in the SLM and would be evidenced as a decrease in the fluorescence signal. However, no sedimentation of the mitochondria was observed (Fig III-9, blue solid line). The sample lacking NBD (Blank) was also constant over time (Figure III-9, red solid line), indicating that the background intensity due to the mitochondria alone is also not reduced. These results were significant because they meant that, for the fluorescence quenching experiments, any observed decrease in the signal would be due to collisions between fluorophore and quencher, and not to sedimentation of the mitochondria.

Alamethicin is a pore-forming antibiotic that will form holes of around 16-20 Å in membranes containing a membrane potential (He et al, 1996), making it useful for forming pores in the mitochondria IM. Upon addition of alamethicin the observed

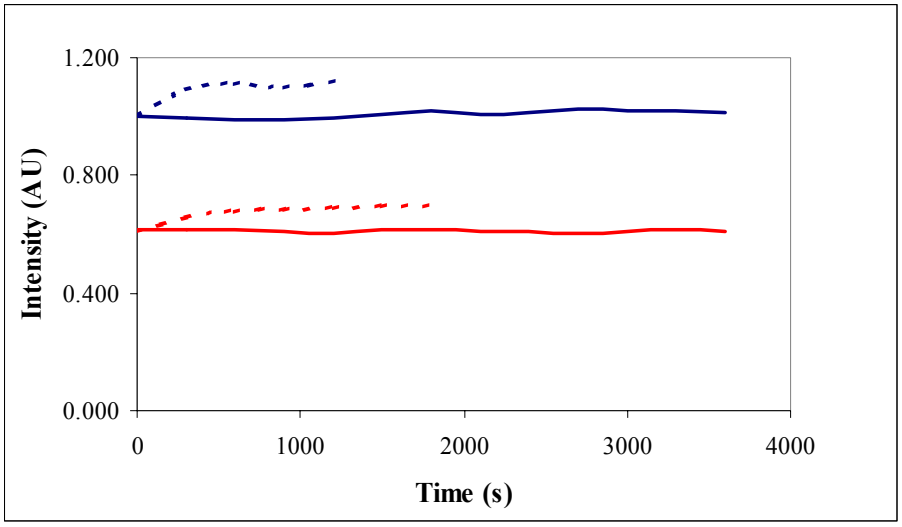

Figure III-9. Time dependence of imported NBD-Su9-DHFR emission. NBD-labeled Su9-DHFR was imported into mitochondria and monitored in the fluorimeter over time at excitation and emission wavelengths of 468 nm and 530 nm, respectively. Time traces were taken before and after treatment with alamethicin (ALA) according to Experimental Procedures. , — Sample (+NBD); ····· , Sample after ALA treatment; —, Blank (-NBD); ····· , Blank after ALA treatment.

signal increases slightly for both the Sample and Blank (Figure III-9, dashed lines). Since this phenomenon is seen for both the Sample (containing NBD) and the Blank (lacking NBD) it appears to be due to an effect of the alamethicin on the mitochondria themselves that results in an increase in the light scattering of the mitochondria.

Evaluation of NBD Probes in the Mitochondrial Matrix

One of the goals of creating this fluorescence system was to evaluate the accessibility of a fluorescent probe to externally added NBD quencher. When the NBD probe was placed along the TOM/TIM23 import pathway, any quenching by the quencher potassium iodide (KI) would indicate accessibility of the probe to the cytosol. These experiments would be performed on different amber mutants of Su9-DHFR to position the NBD probe at different locations along the import pathway. As a first step, the initial experiments had to evaluate the accessibility of the NBD probe when the NBD-Su9-DHFR TAG mutant was fully imported into isolated mitochondria. The iodide ions should not be able to cross the IM; therefore, fully imported NBD-Su9-DHFR is expected to be inaccessible to externally added KI. Indeed, Figure III-10 shows only a small decrease in the NBD fluorescence of full length NBD-Su9-DHFR imported in the absence of MTX. The residual quenching is most likely due to adsorbed NBD-Su9-DHFR proteins that were adsorbed to, but not imported into, the mitochondria, therefore not removed by the high salt wash. To confirm this, the mitochondria were treated with Alamethicin to the KI access to the matrix. Figure III-10 shows that the NBD fluorescence is further decreased in the presence of alamethicin

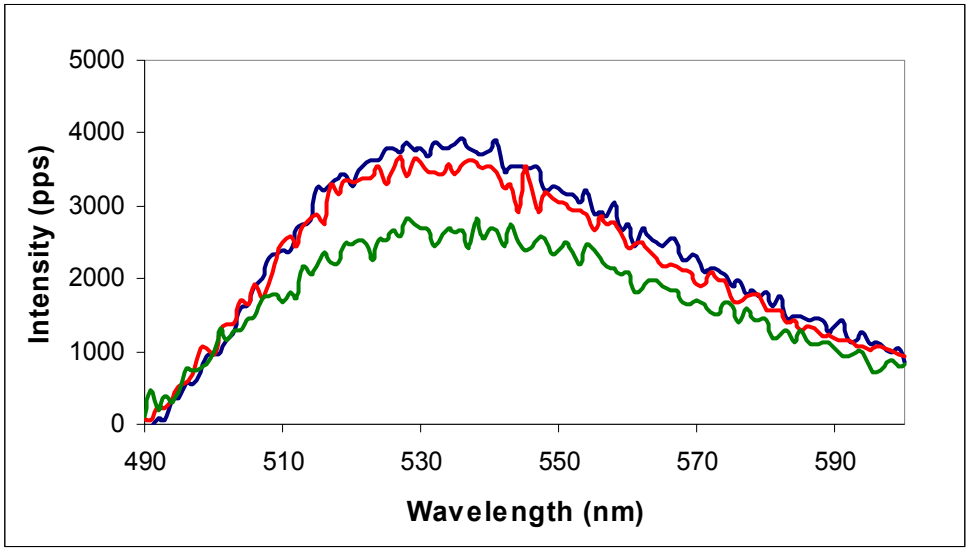

Figure III-10. Accessibility of imported NBD-Su9-DHFR to cytosolic KI. NBD-Su9-DHFR TAG25 was fully imported into isolated mitochondria in the absence of MTX as described in Experimental Methods. NBD emission scans were taken (ex. 468 nm) before (blue) and after (red) addition of 50 mM KI, and after addition of 7.5 µg/mL alamethicin (green).

because the KI can now quench the fully-imported NBD-Su9-DHFR. This, it is possible to evaluate fully-imported NBD-Su9-DHFR in the fluorimeter, and, subsequently, to quench these fully-imported probes by KI after treatment of the mitochondria with alamethicin.

Collisional Quenching of Fully Imported NBD-Su9-DHFR

Fluorescence quenching experiments were performed using NBD-labeled Su9-DHFR TAG mutants that were imported in the absence of MTX. In the absence of MTX the NBD-labeled preproteins would be fully imported into the mitochondrial matrix. Since the collisional quencher (here, iodide ions) cannot diffuse across the IM, the imported NBD-Su9-DHFR should be inaccessible to externally added KI. Therefore, the fluorescence intensity in the presence of quencher (F) would not change much from the initial intensity in the absence of quencher (F_0). The Stern-Volmer equation for quantifying the extent of collisional quenching of fluorescent probes is: $F_0/F = 1 + K_{sv}[Q]$, where Q is the quencher concentration and K_{sv} is the Stern-Volmer quenching constant. A small amount of quenching would result in a small change in F_0/F, and hense in a low Stern-Volmer quenching constant (K_{sv}).

An example of collisional quenching data for fully-imported Su9-DHFR TAG25 in the absence of MTX is shown in Figure III-11, where KI was titrated to a final concentration of 72 mM. As a control for the effect of increasing salt concentration on the imported NBD-Su9-DHFR, KCl was also titrated to a final concentration of 72 mM. Addition of KCl had only a minimal effect on the fluorescence intensity of the sample,

while addition of the quencher KI resulted in an increased amount of collisional quenching, and hence a higher F_0/F ratio (Figure III-11, compare blue line and red line). The "net" Ksv is calculated by subtracting the KCl titration data from the KI titration data (Figure III-11, green line). Alamethicin is added to both the samples titrated with KI and the samples titrated with KCl, and the net F_0/F, after Alamethicin treatment, is calculated; however, since there is only one data point (at 72 mM KI/KCl) linear regression was not performed. Figure III-11 shows that that after Alamethicin treatment, the (F_0/F) increases compared to the value prior to Alamethicin treatment, indicating an increase in quenching by KI due to accessibility of the iodide ions to the NBD probes in the matrix.

As can be seen in Table III-1, all of the Su9-DHFR TAG mutants have net K_{sv} values higher than zero. These data indicate that some fraction of NBD-labeled substrates is adsorbed to the outside surfaces of the mitochondrial membranes and is therefore accessible to the externally added iodide ion quenchers.

To minimize this adsorption phenomenon, a protease digestion was performed after the import step. Upon incubating an import reaction with 50 μg/mL trypsin for 15 min at 0°C prior to sedimenting the mitochondria for spectral analysis, initial K_{sv} constants were lower in some, but not all, cases (Table III-1). Since many of the experiments were performed with low fluorescence intensities, recorded as pulses per second (pps), it was difficult to obtain reproducible results. The collisional quenching experiments recorded in Table III-1 each had a signal of greater than 1200 pps;

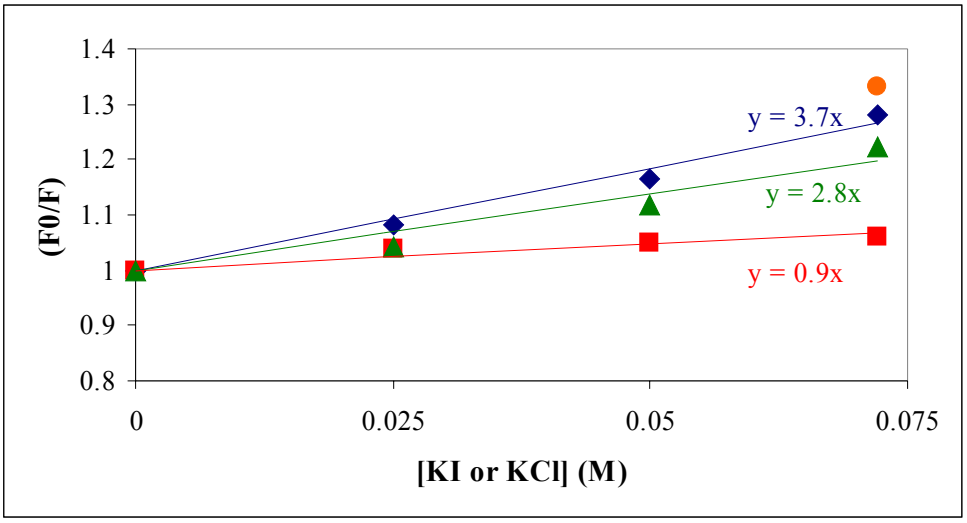

Figure III-11. Matrix NBD-Su9-DHFR accessibility to KI. NBD-Su9-DHFR TAG61 was imported into isolated mitochondria in the absence of MTX and then exposed to either KI (blue) or KCl (red). The "net" accessibility to quenching by iodide ions was calculated by subtracting the KI data from the KCl data, and is shown in this graph in green. Linear regression was performed on each data set, with the intercept set to equal 1, and the slopes of each line (the Stern-Volmer quenching constant, or K_{sv}) is recorded on the graph in the same color as the corresponding data/line. After titration with KI or KCl, the samples were treated with 5 µg/mL alamethicin. The net accessibility to quenching by iodide ions after alamethicin treatment is shown in orange. Because only one point was recorded linear regression was not performed.

Table III-1. Stern-Volmer quenching constants for Su9-DHFR TAG mutants (- MTX)

			- Trypsin		
TAG	**n[b]**	**pps[a]**	**K_{sv}, I (M^{-1})***	**K_{sv}, Cl (M^{-1})***	**K_{sv} net (M^{-1})***
25	3	4400	4.4 +/- 0.5	2.0 +/- 0.7	2.6 +/- 0.9
33	5	2900	4.4 +/- 0.5	1.8 +/- 0.6	2.8 +/- 0.6
50	2	3300	3.1 +/- 0.8	0.5 +/- 0.5	2.5 +/- 0.2
61	3	4050	3.2 +/- 0.5	1.2 +/- 0.5	1.8 +/- 0.8
70	1	2400	1.5	-0.2	1.6
			+ Trypsin		
TAG	**n[b]**	**pps[a]**	**K_{sv}, I (M^{-1})***	**K_{sv}, Cl (M^{-1})***	**K_{sv} net (M^{-1})***
40	4	3100	2.5 +/- 0.5	0.6 +/- 0.7	1.8 +/- 1.0
61	1	1700	1	0.3	0.3

[a] pps: pulses per second, averaged over n repetitions

[b] n, number of repetitions

* Reported as averages, standard deviations over n repetitions

quenching experiments with intensities of less than 1200 pps were not included, since the signals were too low to obtain reproducible quenching data.

Collisional Quenching of Su9-DHFR Import Intermediates

Fluorescence quenching experiments were also performed for NBD-Su9-DHFR imported in the presence of MTX, both with and without a trypsin digestion of the import intermediates prior to spectral analysis (Table III-2). For the quenching experiments performed in the presence of MTX, and without a trypsin digestion prior to spectral analysis, the net K_{sv} values are similar for all of the TAG constructs, and all higher than zero, indicating a population of NBD-Su9-DHFR polypeptides is adsorbed to the mitochondria. For the quenching experiments performed in the presence of MTX and with a trypsin digestion prior to spectral analysis, the net K_{sv} values are generally lower. However, some constructs have data for only one experiment, since experiments with fluorescence signals less than 1200 pps were not included in the data set. Some of the data for the constructs gather under conditions where the NBD-Su9-DHFR was imported in the presence of MTX and was subjected to a trypsin digestion indicated negative net K_{sv} values as well, such as the TAG50 and TAG70 construct. These results are most likely due to small fluorescence intensities. More repetitions, performed on samples with higher intensities, would allow for a more accurate net K_{sv} value to be obtained.

However, data interpretation is complicated for the Su9-DHFR import intermediates by the fact that there are multiple populations of NBD-Su9-DHFR nascent

Table III-2. Stern-Volmer quenching constants for Su9-DHFR TAG mutants (+ MTX)

TAG	n[b]	pps[a]	- Trypsin K_{sv}, I (M^{-1})*	K_{sv}, Cl (M^{-1})*	K_{sv} net (M^{-1})*
25	4	3000	3.1 +/- 0.9	0.9 +/- 0.5	2.1 +/- 0.7
50	3	1800	3.3 +/- 2.7	1.1 +/- 0.4	2.2 +/- 2.2
61	2	3750	4.5 +/- 1.6	2.0 +/- 0.3	2.4 +/- 1.0
TAG	**n[b]**	**pps[a]**	**+ Trypsin K_{sv}, I (M^{-1})***	**K_{sv}, Cl (M^{-1})***	**K_{sv} net (M^{-1})***
40	2	2150	2.6 +/- 1.6	1.7 +/- 0.4	0.1 +/- 1.1
50	1	2400	1.8	2	-0.2
61	1	1300	4.4	2.8	1.8
70	1	1900	1.6	3.4	-3.8

[a] pps: pulses per second, averaged over n repetitions

[b] n, number of repetitions

* Reported as averages, standard deviations over n repetitions

chains. As seen in Figure III-3, there is a small population of mature, imported Su9-DHFR, even in the presence of MTX, though most proteins are trapped at the TOM complex. After trypsin digestion, the amount of precursor protein is diminished, but two populations of Su9-DHFR nascent chains still exist – the import intermediates, bound by MTX, and the mature protein, not bound to MTX. The fate of the NBD- labeled presequences removed by MPP is unknown, but it is presumed that the NBD probes remain inside the mitochondrial matrix. Because there are NBD-Su9-DHFR polypeptides both bound as import intermediates and fully imported, their accessibilities to the KI quencher may differ. If they do, the observed fluorescence signal will reflect the weighted molar averages of the quenching experienced by the two populations.

It is possible, however, to compare overall K_{sv} results for the Su9-DHFR TAG mutants in the presence and absence of MTX. For the Su9-DHFR TAG61 construct, the overall K_{sv} value is around 0.3 M^{-1} in the absence of MTX (fully imported), and is around 1.8 M^{-1} in the presence of MTX (import intermediate). The overall K_{sv} is also lower for the TAG40 import intermediate (0.1 M^{-1}), compared to the fully imported construct (1.8 M^{-1}). However, the average K_{sv} values for all of these constructs are within one standard deviation, so the –MTX and +MTX results are most likely not statistically different from each other. This would suggest that the NBD probes placed along the import pathway during the experiments +MTX are no more accessible to externally-added iodide ions that the probes fully imported into the matrix in the absence of MTX. More repetitions, with more TAG positions, would be required to verify this supposition.

Evaluation of the Environment of the NBD probe in the Su9-DHFR Import Intermediates

After each fluorescence quenching experiment is completed, the samples are analyzed for the amount of [^{14}C] radioactivity to determine the number of NBD probes contained in each sample. A ratio is calculated between the observed net fluorescence intensity (pulses per second, pps) and the radioactivity (counts per minute, cpm), referred to as the pps/cpm ratio, that provides an indication of the environment of the NBD probe. When two different experiments have similar pps/cpm ratios, the NBD probes are likely in the same environment. The average pps/cpm ratios for the NBD-Su9-DHFR TAG mutants are listed in Table III-3. Since the pps/cpm ratios for various mutants are very similar, it appears that for each construct the NBD probe is in the same environment in each intermediate. The pps/cpm ratios for the different NBD-Su9-DHFR TAG mutants were higher than that of the εNBD-[^{14}C]Lys-tRNA^{amb}, as well as for the εNBD-[^{14}C]Lys after hydrolysis away from the tRNA moiety. The lower pps/cpm ratio for the NBD probe while attached to the tRNA is most likely due to an alteration in NBD spectral properties caused by the stacking of the NBD ring and tRNA bases. Hydrolysis of the NBD probe away from the tRNA resulted in a higher pps/cpm ratio, although it is still not as high as for the NBD-Su9-DHFR TAG mutants. The most likely reason for this discrepancy is the possibility that there are NBD probes in different environments (aqueous and nonpolar) for both the fully-imported (-MTX) and intermediate (+MTX)

Table III-3. Pps/cpm ratios for Su9-DHFR TAG mutants

TAG	MTX	n[b]	pps/cpm[a]
25	+	4	5.7 +/- 0.9
	-	4	5.2 +/- 0.1
33	+	5	5.3 +/- 1.0
	-	-	-
40	+	2	4.2 +/- 0.7
	-	4	4.2 +/- 1.8
50	+	3	5.4 +/- 0.3
	-	2	3.8 +/- 2.6
61	+	2	5.8 +/- 0.1
	-	7	5.7 +/- 0.5
70	+	1	5.6
	-	2	3.7 +/- 0.9
NBD-[^{14}C]Lys tRNA^{amb}[c]		2	1
NBD-[^{14}C]Lys[d]		1	2

[a] Pps readings were taken at excitation and emission wavelengths of 468 nm and 530 nm, respectively. After spectral measurements were taken, 50% of sample was removed, added to a Triton-based scintillation cocktail, and counted using a liquid scintillation counter.

[b] number of repetitions

[c] NBD-[^{14}C]Lys-tRNA^{amb} was diluted into SLM Buffer intensity read as for the NBD-Su9-DHFR readings. 100% of the sample was removed, added to a Triton-based scintillation cocktail, and counted as above.

[d] Treated the same as in [c], except the NBD-[^{14}C]Lys was hydrolyzed from the tRNA by heating at 37 C for 1 h prior to spectral analysis.

NBD-Su9-DHFR polypeptides. The resultant pps/cpm ratio is a weighted average of the probes in an aqueous environment, which have a low pps/cpm ratio (Crowley et al, 1993) and the probes in a nonpolar environment, which have a high pps/cpm ratio. Without the use of fluorescence lifetime analysis to determine the molar fraction of NBD probes in each environment, we cannot assess the distribution of NBD probes in aqueous or nonpolar environments. Previous electrophysiological and cryo EM data suggest that Tim23 forms an aqueous channel (Truscott et al, 2001), but no experiments have examined the environment of protein substrates except for the above fluorescence measurements. But while the data summarized in Table III-3 indicate that the NBD environments do not change significantly at different locations along the import pathway before or after being fully imported, further experiments will be necessary to accurately characterize probe locale.

Location of Su9-DHFR Probe Positions Along the Import Pathway

To identify the location of each Su9-DHFR TAG mutant along the import pathway, chemical crosslinking was employed. Su9-DHFR Cys mutants were translated and imported into isolated mitochondria as described in Experimental Methods, and then treated with the homobifunctional cysteine-cysteine crosslinker BMH. The BMH will create a covalent bond between the cysteine residue in the Su9-DHFR construct and any cysteine residue of a neighboring protein that is within reach of the 16 Å BMH spacer arm. Figures III-12 and III-13 show the BMH crosslinking data for the WT Su9-DHFR as well as the Cys mutants 8, 20, 25, 40, and 60. The WT construct, which contains only

the native cysteine residue at position 79, appears to form a prominent covalent adduct with a molecular mass near 60 kDa in both the presence and absence of MTX (Figure III-12, lanes 3 and 5). This same covalent adduct is seen for each Su9-DHFR TAG construct (marked in each lane with a >) and is most likely an artifact caused by radioactive material being washed ahead of the relatively large bolus of proteins in the gel at that location.

However, different crosslinking patterns were observed for the Su9-DHFR Cys mutants, indicating that the formation of the covalent adducts seen depends on the location of the second cysteine residue in the Su9-DHFR polypeptide. The Su9-DHFR constructs with cysteines at positions 8, 25, 40 and 60 all form a large molecular mass adduct of approximately 85 kDa (Figure III-12, lanes 8 and 10; Figure III-13, lanes 3, 5, 8, 10, 13, and 15, marked with an asterisk). By subtracting the molecular weight of the Su9-DHFR construct (approximately 30 kDa), the molecular mass of the adduct is estimated to be near 55 kDa. This common crosslinking target is most likely Tim50, a protein thought to be near substrates importing using the TIM23 Complex. The Su9-DHFR Cys8 construct also shows other crosslinking adducts seen for both the +MTX and –MTX reactions, of sizes 125 kDa, 72 kDa, and 50 kDa (Figure III-12, lanes 8 and 10, marked with ^, •, and °, respectively).

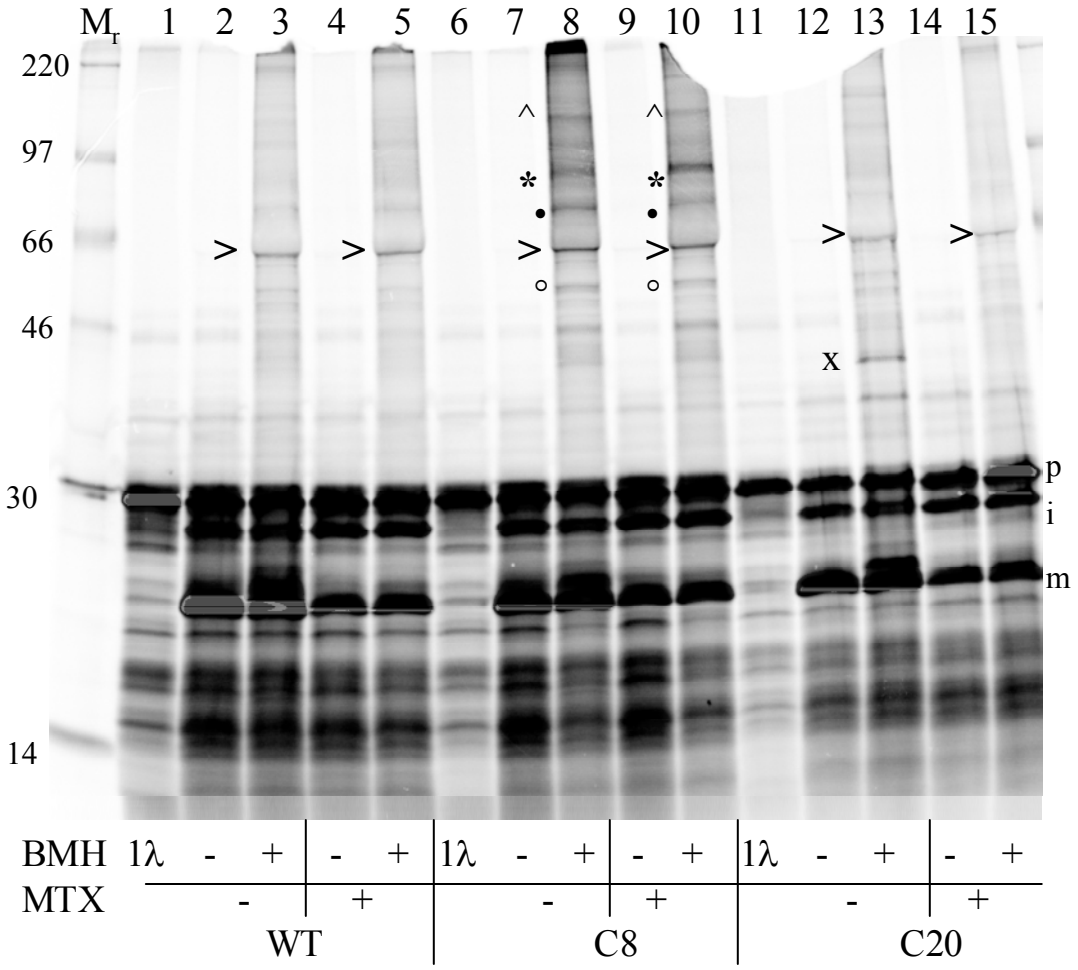

Figure III-12. Chemical crosslinking of Su9-DHFR Cys8 and Cys20. Su9-DHFR Cys mutants were translated, imported, and reacted with BMH as described in Experimental Methods. Each crosslinking reaction was performed in the presence and absence of MTX. The construct used for the reaction is indicated below the appropriate lanes. 1λ refers to the amount of the translation reaction loaded directly onto the gel. The > identifies a background band that appears in every lane containing BMH (lanes 3, 5, 8, 10, 13, and 15). For the Su9-DHFR Cys8 construct, many covalent adducts are seen in lanes 8 and 10. The bands marked with a ^ denote a covalent adduct of around 125 kDa, while the bands marked with an * denote a larger covalent adduct of around 85 kDa. Smaller covalent adducts marked with • and ° have molcular masses of around 72 kDa and 50 kDa, respectively. For the Su9-DHFR Cys20 construct in the absence of MTX, a covalent adduct with a molecular mass of 40 kDa is seen (in lane 13, marked with an x). p, Su9-DHFR precursor; i, Su9-DHFR intermediate form; m, Su9-DHFR mature form.

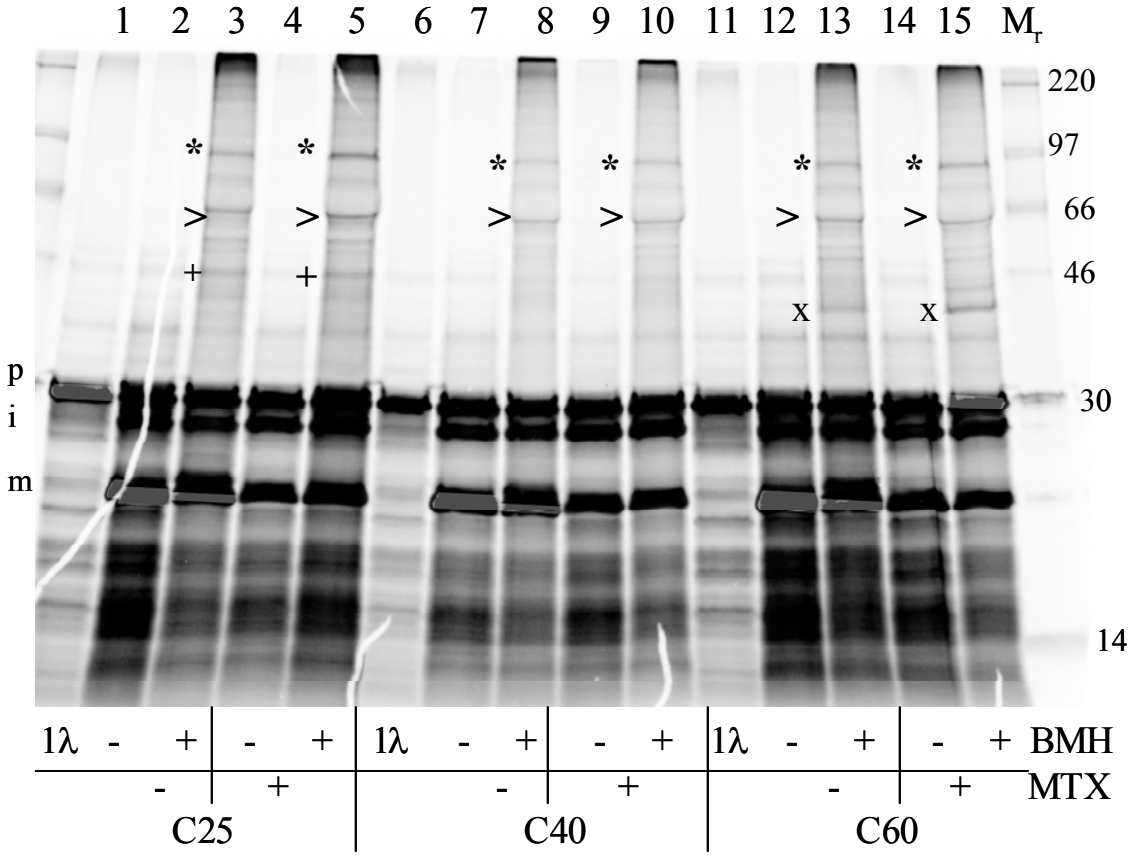

Figure III-13. Chemical crosslinking of Su9-DHFR Cys25 and Cys40, and Cys60. Su9-DHFR Cys mutants were translated, imported, and reacted with BMH as described in Experimental Methods. Each crosslinking reaction was performed in the presence and absence of MTX. The construct used for the reaction is indicated below the appropriate lanes. 1λ refers to the amount of the translation reaction loaded directly onto the gel. The > refers to a background band that appears in every lane containing BMH (lanes 3, 5, 8, 10, 13, and 15). The bands marked with an asterisk in lanes 3, 5, 8 , 10, 13 and 15 denote a covalent adduct also seen for each construct, with a molecular mass of 90 kDa. The bands marked with a X in lanes 13 and 15 denote a covalent adduct of around 40 kDa seen for the Su9-DHFR Cys60 construct. A covalent adduct of around 46 kDa is seen for the Su9-DHFR Cys25 construct (lanes 3 and 5, marked with a +). p, Su9-DHFR precursor; i, Su9-DHFR intermediate form; m, Su9-DHFR mature form.

Other crosslinking adducts vary with the position of the second cysteine. A covalent adduct of around 46 kDa was seen for the Su9-DHFR Cys25 construct, both in the presence and absence of MTX (Figure III-13, lanes 3 and 5, marked with a +). After correcting for the molecular mass of the Su9-DHFR precursor, the mass of the adduct is around 16 kDa, which could indicate that the identity of the adduct is Tim17, another component of the TIM23 complex. A small covalent adduct of approximately 42 kDa is observed for Su9-DHFR Cys60 (Figure III-13, lanes 13 and 15 (marked with an x)), but not for the other constructs. After correcting for the molecular mass of the Su9-DHFR precursor, the mass of the adduct is estimated to be around 12 kDa, suggesting the identity of the adduct could be Tim14/Pam16, an IM member of the PAM Complex. Immunoprecipitations against TOM, IMS, and TIM23 components will be required to identify the crosslinking targets.

It should be noted that several of the covalent adducts do not appear to be dependent on the presence of MTX (i.e., the presence of import intermediates). However, the presence of an intermediate band, denoted with an i in Figures III-12 and III-13, is seen for all imported constructs, even in the absence of MTX. This intermediate band is seen when the Su9-DHFR construct is only imported into the matrix far enough for the first MPP site to be cleaved. Since these Su9-DHFR polypeptides are not completely imported (that is, they have not reached the mature length), it seems likely that they constitute a population of import intermediates that might crosslink to the TOM and TIM23 import components.

While the lack of MTX dependence in the chemical crosslinking results is disconcerting, in some respects it correlates with previous data showing the relatively small fraction of Su9-DHFR that is bound by MTX in a trypsin-resistant fashion (see Figure III-3, lane 3). The fact that for each import reaction the fraction of Su9-DHFR processed to the mature (m) form is less in the presence of MTX than in the absence of MTX indicates that the MTX is binding a portion of the translated Su9-DHFR polypeptides. Since such a small amount of the mitochondria-associated Su9-DHFR is forming MTX-bound import intermediates the observed crosslinking efficiency would be expected to be very low. The crosslinking bands seen in Figures III-12 and III-13 are likely the result of the Su9-DHFR intermediate (i) population, which appear to remain constant in the presence and absence of MTX. However the import intermediates are formed, it does follow that the pattern of chemical crosslinking with BMH does change with different Su9-DHFR Cys mutants, indicating that the covalent adducts seen are dependent on the location of the second cysteine residue.

CHAPTER IV

CONCLUSIONS

The experiments performed in this thesis revealed that it is possible to use fluorescence spectroscopy to examine protein import into mitochondria. First, it was found that an NBD fluorescent probe could be site-specifically incorporated into the model matrix protein Su9-DHFR using the amber suppressor tRNA system developed in the Johnson lab (Flanagan et al, 2003). Second, *in vitro* import experiments revealed that the presence of the NBD probe on the preprotein does not interfere with the ability of the preprotein to be efficiently imported into the mitochondrial matrix. Third, fluorescence collisional quenching experiments revealed that the NBD-Su9-DHFR preproteins fully imported into the mitochondrial matrix are inaccessible to externally-added iodide quencher, but can be quenched by the iodide ions after the mitochondria are treated with the pore-forming antibiotic alamethicin. Fourth, Su9-DHFR import intermediates could be generated with the NBD-Su9-DHFR preproteins using the folate analog methotrexate, and these import intermediates could also be using for collisional quenching experiments. Fifth, the environment of the NBD probe, as evaluated by the pps/cpm ratio, does not appear to vary with the position of the NBD probe along the import pathway. The pps/cpm ratio was also the same for each probe position both as an import intermediate and as a fully imported protein in the mitochondrial matrix. Taken separately, each one of these statements reflects a small step towards setting up the mitochondrial import system for fluorescence analysis. However, taken together, these

data show that it is possible to analyze mitochondrial import via fluorescence techniques. Further, site-specific incorporation of a fluorescent probe into the Su9-DHFR preprotein allows for the possibility of examination of a specific location along the import pathway, such as the TOM complex or the TIM23 complex.

One of the two main difficulties that arose while adapting the mitochondrial import system for fluorescence studies was low signal intensity. *In vitro* mitochondrial import is, on average, about 30% efficient, which means that about 30% of the translated preproteins are actually processed to their mature form. Since there is only one NBD probe per preprotein, this low import phenomenon results in a small amount of fluorescent probes fully imported into the mitochondria. Also, the mitochondria themselves contain a lot of background fluorescence, which further decreases the signal to noise ratio. Many different optimizations were attempted to either boost the signal, by further increasing in vitro import efficiency, or lower the noise, by limiting the amount of mitochondrial protein in the sample cuvettes, but no significant effects were seen with respect to higher fluorescence intensity. Import experiments using a different fluorescent probe were also attempted. The [^{14}C]Lys-tRNA^{amb} was modified with the BODIPY fluorophore (4,4-difluoro-4-bora-3a, 4a-diaza-s-indacene, Molecular Probes). The BODIPY probe has a high quantum yield, and hence a relatively high fluorescence intensity per probe. However, it was found to be impractical to use the probe for collisional quenching experiments because very little suppression of the Su9-DHFR TAG mutants was observed due to the larger size of BODIPY than of NBD. The BODIPY probe is also not very environmentally sensitive; thus, we could not use this

probe to measure the environment (aqueous or nonpolar) of the preprotein during import. To increase the signal to noise ratio of the Su9-DHFR import intermediates, one option is to overexpress and purify Su9-DHFR from *E. coli*. This purified Su9-DHFR could then be labeled with NBD, and a higher concentration of purified NBD-Su9-DHFR could be used in import incubations. This technique of importing overexpressed protein has been used before (Dembowski et al, 2001) and it may provide a viable alternative to importing *in vitro*-translated Su9-DHFR.

The second primary difficulty in doing the fluorescence quenching experiments with Su9-DHFR import intermediates was interpreting spectral data from samples containing mixed populations of precursor and mature protein. As mentioned briefly in Chapter III, after importing the Su9-DHFR TAG mutants into mitochondria in the presence of MTX, three different populations were generated: the import intermediates, which were bound by MTX and which spanned the OM and IM; the fully imported and processed DHFR, which was not bound to MTX; and the Su9-DHFR preproteins adsorbed to the outside of the mitochondria, which might or might not be bound to MTX. While a mild trypsin digestion reduced the number of adsorbed nascent chains, two populations still remained, and often the fraction of Su9-DHFR import intermediates was small, compared to that in the matrix. These mature proteins no longer contain the NBD-labeled Su9 presequence, and the fate of the presequences after processing by MPP is as yet unknown. Thus, analysis of the spectral data is further complicated by uncertainty about the location of released fluorescent presequences. Since different probe populations may have different accessibilities to the externally added iodide ion

quenchers, ascertaining the extent of iodide ion quenching of individual species is difficult. Accurate interpretation of collisional quenching, fluorescence lifetime, and other spectral data require either a homogeneous population of import intermediates, which we were unable to achieve, or a means to establish biochemically the distribution of fluorophores among different locations or structural states (Johnson, 2005).

Despite this disappointment, the body of work contained in this thesis constitutes the first evidence that using fluorescence spectroscopy to analyze protein import into isolated mitochondria is feasible. Further optimizations of the import conditions, such as the length of Su9 presequence, possible overexpression of the Su9-DHFR preprotein, and a "better" fluorescent probe that is efficiently incorporated into the preprotein and has a higher quantum yield than NBD, might allow the original specific aims of the project to be fulfilled. Another possibility, now that the import conditions are optimized for fluorescence analysis, would be to perform imports of a fluorescent-labeled translocase component, such as mtHsp70, or Tim23, and analyze its interactions with the other components of its translocase by changes in the lifetime of the fluorophore, its ability to be collisionally quenched by an externally-added quencher, or even its proximity to another fluorescent-labeled component (FRET analysis). All of these possibilities are conceivable, based on the viability, shown here, of importing a fluorescent preprotein into mitochondria. Despite the experimental challenges that remain, this spectroscopic approach will ultimately contribute significantly to our understanding of mitochondrial protein import pathways.

REFERENCES

Abe, Y., Shodai, T., Muto, T., Mihara, K., Torii, H., Nishikawa, S., Endo, T., and Kohda, D. (2000). Structural basis of presequence recognition by the mitochondrial protein import receptor Tom20. Cell *100*, 551-560.

Adrain, C., and Martin, S. J. (2001). The mitochondrial apoptosome: a killer unleashed by the cytochrome seas. Trends Biochem Sci *26*, 390-397.

Ahting, U., Theiffry, M., Engelhardt, H., Hegerl, R., Neupert, W., and Nussberger, S. (2001). Tom40, the pore-forming component of the protein-conducting TOM channel in the outer membrane of mitochondria. J Cell Biol *153*, 1151-1160.

Ahting, U., Thun, C., Hegerl, R., Typke, D., Nargang, F. E., Neupert, W., and Nussberger, S. (1999). The TOM core complex: the general protein import pore of the outer membrane of mitochondria. J Cell Biol *147*, 959-968.

Alberts, B. B., Bray, D., Lewis, J., Raff, M., Roberts, K., Watson, J.D. (1994). Molecular Biology of the Cell, 3rd ed. (New York: Garland Publishing).

Allen, S., Balabanidou, V., Sideris, D. P., Lisowsky, T., and Tokatlidis, K. (2005). Erv1 mediates the Mia40-dependent protein import pathway and provides a functional link to the respiratory chain by shuttling electrons to cytochrome c. J Mol Biol *353*, 937-944.

Bauer, M., Behrens, M., Esser, K., Michaelis, G., and Pratje, E. (1994). PET1402, a nuclear gene required for proteolytic processing of cytochrome oxidase subunit 2 in yeast. Mol Gen Genet *245*, 272-278.

Bauer, M. F., Sirrenberg, C., Neupert, W., and Brunner, M. (1996). Role of Tim23 as voltage sensor and presequence receptor in protein import into mitochondria. Cell *87*, 33-41.

Bolliger, L., Junne, T., Schatz, G., and Lithgow, T. (1995). Acidic receptor domains on both sides of the outer membrane mediate translocation of precursor proteins into yeast mitochondria. EMBO J *14*, 6318-6326.

Bonnefoy, N., Chalvet, F., Hamel, P., Slonimski, P. P., and Dujardin, G. (1994). OXA1, a Saccharomyces cerevisiae nuclear gene whose sequence is conserved from prokaryotes to eukaryotes controls cytochrome oxidase biogenesis. J Mol Biol *239*, 201-212.

Chacinska, A., Lind, M., Frazier, A. E., Dudek, J., Meisinger, C., Geissler, A., Sickmann, A., Meyer, H. E., Truscott, K. N., Guiard, B.*, et al.* (2005). Mitochondrial

presequence translocase: switching between TOM tethering and motor recruitment involves Tim21 and Tim17. Cell *120*, 817-829.

Chacinska, A., Pfannschmidt, S., Wiedemann, N., Kozjak, V., Sanjuan Szklarz, L. K., Schulze-Specking, A., Truscott, K. N., Guiard, B., Meisinger, C., and Pfanner, N. (2004). Essential role of Mia40 in import and assembly of mitochondrial intermembrane space proteins. EMBO J *23*, 3735-3746.

Craig, E. A., Kramer, J., Shilling, J., Werner-Washburne, M., Holmes, S., Kosic-Smithers, J., and Nicolet, C. M. (1989). SSC1, an essential member of the yeast HSP70 multigene family, encodes a mitochondrial protein. Mol Cell Biol *9*, 3000-3008.

Crowley, K. S., Liao, S., Worrell, V. E., Reinhart, G. D., and Johnson, A. E. (1994). Secretory proteins move through the endoplasmic reticulum membrane via an aqueous, gated pore. Cell *78*, 461-471.

Crowley, K. S., Reinhart, G. D., and Johnson, A. E. (1993). The signal sequence moves through a ribosomal tunnel into a noncytoplasmic aqueous environment at the ER membrane early in translocation. Cell *73*, 1101-1115.

Curran, S. P., Leuenberger, D., Oppliger, W., and Koehler, C. M. (2002a). The Tim9p-Tim10p complex binds to the transmembrane domains of the ADP/ATP carrier. EMBO J *21*, 942-953.

Curran, S. P., Leuenberger, D., Schmidt, E., and Koehler, C. M. (2002b). The role of the Tim8p-Tim13p complex in a conserved import pathway for mitochondrial polytopic inner membrane proteins. J Cell Biol *158*, 1017-1027.

Daum, G., Bohni, P. C., and Schatz, G. (1982). Import of proteins into mitochondria. Cytochrome b2 and cytochrome c peroxidase are located in the intermembrane space of yeast mitochondria. J Biol Chem *257*, 13028-13033.

Davis, A. J., Ryan, K. R., and Jensen, R. E. (1998). Tim23p contains separate and distinct signals for targeting to mitochondria and insertion into the inner membrane. Mol Biol Cell *9*, 2577-2593.

Davis, A. J., Sepuri, N.B., Holder, J., Johnson, A.E., and Jensen, R.E., (2000). Two intermembrane space TIM complexes interact with different domains of Tim23p during its import into mitochondria. J Cell Biol *150*, 1271-1282.

Dekker, P. J., Keil, P., Rassow, J., Maarse, A. C., Pfanner, N., and Meijer, M. (1993). Identification of MIM23, a putative component of the protein import machinery of the mitochondrial inner membrane. FEBS Lett *330*, 66-70.

Dekker, P. J., Martin, F., Maarse, A. C., Bomer, U., Muller, H., Guiard, B., Meijer, M., Rassow, J., and Pfanner, N. (1997). The Tim core complex defines the number of mitochondrial translocation contact sites and can hold arrested preproteins in the absence of matrix Hsp70-Tim44. EMBO J *16*, 5408-5419.

Dell, V. A., Miller, D. L., and Johnson, A. E. (1990). Effects of nucleotide- and aurodox-induced changes in elongation factor Tu conformation upon its interactions with aminoacyl transfer RNA. A fluorescence study. Biochemistry *29*, 1757-1763.

Dembowski, M., Kunkele, K., Nargang, F.E., Neupert, W., and Rapaport, D. (2001). Assembly of Tom6 and Tom7 into the TOM core complex of *Neurospora crassa*. J Biol Chem *276*, 17679-17685.

Dietmeier, K., Honlinger, A., Bomer, U., Dekker, P. J., Eckerskorn, C., Lottspeich, F., Kubrich, M., and Pfanner, N. (1997). Tom5 functionally links mitochondrial preprotein receptors to the general import pore. Nature *388*, 195-200.

Donzeau, M., Kaldi, K., Adam, A., Paschen, S., Wanner, G., Guiard, B., Bauer, M. F., Neupert, W., and Brunner, M. (2000). Tim23 links the inner and outer mitochondrial membranes. Cell *101*, 401-412.

D'Silva, P., Liu, Q., Walter, W., and Craig, E. A. (2004). Regulated interactions of mtHsp70 with Tim44 at the translocon in the mitochondrial inner membrane. Nat Struct Mol Biol *11*, 1084-1091.

D'Silva, P. D., Schilke, B., Walter, W., Andrew, A., and Craig, E. A. (2003). J protein cochaperone of the mitochondrial inner membrane required for protein import into the mitochondrial matrix. Proc Natl Acad Sci U S A *100*, 13839-13844.

Eilers, M., and Schatz, G. (1986). Binding of a specific ligand inhibits import of a purified precursor protein into mitochondria. Nature *322*, 228-232.

Emtage, J. L., and Jensen, R. E. (1993). MAS6 encodes an essential inner membrane component of the yeast mitochondrial protein import pathway. J Cell Biol *122*, 1003-1012.

Erickson, A. H., and Blobel, G. (1983). Cell-free translation of messenger RNA in a wheat germ system. Methods Enzymol *96*, 38-50.

Esaki, M., Kanamori, T., Nishikawa, S., Shin, I., Schultz, P. G., and Endo, T. (2003). Tom40 protein import channel binds to non-native proteins and prevents their aggregation. Nat Struct Biol *10*, 988-994.

Flanagan, J. J., Chen, J. C., Miao, Y., Shao, Y., Lin, J., Bock, P. E., and Johnson, A. E. (2003). Signal recognition particle binds to ribosome-bound signal sequences with fluorescence-detected subnanomolar affinity that does not diminish as the nascent chain lengthens. J Biol Chem *278*, 18628-18637.

Frazier, A. E., Dudek, J., Guiard, B., Voos, W., Li, Y., Lind, M., Meisinger, C., Geissler, A., Sickmann, A., Meyer, H. E*., et al.* (2004). Pam16 has an essential role in the mitochondrial protein import motor. Nat Struct Mol Biol *11*, 226-233.

Gakh, O., Cavadini, P., and Isaya, G. (2002). Mitochondrial processing peptidases. Biochim Biophys Acta *1592*, 63-77.

Gartner, F., Bomer, U., Guiard, B., and Pfanner, N. (1995). The sorting signal of cytochrome b2 promotes early divergence from the general mitochondrial import pathway and restricts the unfoldase activity of matrix Hsp70. EMBO J *14*, 6043-6057.

Geissler, A., Chacinska, A., Truscott, K. N., Wiedemann, N., Brandner, K., Sickmann, A., Meyer, H. E., Meisinger, C., Pfanner, N., and Rehling, P. (2002). The mitochondrial presequence translocase: an essential role of Tim50 in directing preproteins to the import channel. Cell *111*, 507-518.

Geissler, A., Rassow, J., Pfanner, N., and Voos, W. (2001). Mitochondrial import driving forces: enhanced trapping by matrix Hsp70 stimulates translocation and reduces the membrane potential dependence of loosely folded preproteins. Mol Cell Biol *21*, 7097-7104.

Gentle, I., Gabriel, K., Beech, P., Waller, R., and Lithgow, T. (2004). The Omp85 family of proteins is essential for outer membrane biogenesis in mitochondria and bacteria. J Cell Biol *164*, 19-24.

Glick, B. S., Brandt, A., Cunningham, K., Muller, S., Hallberg, R. L., and Schatz, G. (1992). Cytochromes c1 and b2 are sorted to the intermembrane space of yeast mitochondria by a stop-transfer mechanism. Cell *69*, 809-822.

Hahne, K., Haucke, V., Ramage, L., and Schatz, G. (1994). Incomplete arrest in the outer membrane sorts NADH-cytochrome b5 reductase to two different submitochondrial compartments. Cell *79*, 829-839.

Hamman, B. D., Chen, J. C., Johnson, E. E., and Johnson, A. E. (1997). The aqueous pore through the translocon has a diameter of 40-60 A during cotranslational protein translocation at the ER membrane. Cell *89*, 535-544.

Hamman, B. D., Hendershot, L. M., and Johnson, A. E. (1998). BiP maintains the permeability barrier of the ER membrane by sealing the lumenal end of the translocon pore before and early in translocation. Cell *92*, 747-758.

He, K., Ludtke, S. J., Worcester, D. L., and Huang, H. W. (1996). Neutron scattering in the plane of membranes: structure of alamethicin pores. Biophys J *70*, 2659-2666.

Hell, K., Herrmann, J., Pratje, E., Neupert, W., and Stuart, R. A. (1997). Oxa1p mediates the export of the N- and C-termini of pCoxII from the mitochondrial matrix to the intermembrane space. FEBS Lett *418*, 367-370.

Hell, K., Herrmann, J. M., Pratje, E., Neupert, W., and Stuart, R. A. (1998). Oxa1p, an essential component of the N-tail protein export machinery in mitochondria. Proc Natl Acad Sci U S A *95*, 2250-2255.

Hell, K., Neupert, W., and Stuart, R. A. (2001). Oxa1p acts as a general membrane insertion machinery for proteins encoded by mitochondrial DNA. EMBO J *20*, 1281-1288.

Hill, K., Model, K., Ryan, M. T., Dietmeier, K., Martin, F., Wagner, R., and Pfanner, N. (1998). Tom40 forms the hydrophilic channel of the mitochondrial import pore for preproteins [see comment]. Nature *395*, 516-521.

Hoppins, S. C., and Nargang, F. E. (2004). The Tim8-Tim13 complex of *Neurospora crassa* functions in the assembly of proteins into both mitochondrial membranes. J Biol Chem *279*, 12396-12405.

Horwich, A. L., Kalousek, F., Mellman, I., and Rosenberg, L. E. (1985). A leader peptide is sufficient to direct mitochondrial import of a chimeric protein. EMBO J *4*, 1129-1135.

Hurt, E. C., Pesold-Hurt, B., and Schatz, G. (1984). The cleavable prepiece of an imported mitochondrial protein is sufficient to direct cytosolic dihydrofolate reductase into the mitochondrial matrix. FEBS Lett *178*, 306-310.

Hwang, S., Jascur, T., Vestweber, D., Pon, L., and Schatz, G. (1989). Disrupted yeast mitochondria can import precursor proteins directly through their inner membrane. J Cell Biol *109*, 487-493.

Jensen, R., and Dunn, C. (2002). Protein import into and across the mitochondrial inner membrane: role of the TIM23 and TIM22 translocons. Biochim Biophys Acta *1592*, 25.

Johnson, A. E. (2005). Fluorescence approaches for determining protein conformations, interactions and mechanisms at membranes. Traffic *6*, 1078-1092.

Johnson, A. E., Adkins, H. J., Matthews, E. A., and Cantor, C. R. (1982). Distance moved by transfer RNA during translocation from the A site to the P site on the ribosome. J Mol Biol *156*, 113-140.

Johnson, A. E., and van Waes, M. A. (1999). The translocon: a dynamic gateway at the ER membrane. Annu Rev Cell Dev Biol *15*, 799-842.

Johnson, A. E., Woodward, W. R., Herbert, E., and Menninger, J. R. (1976). Nepsilon-acetyllysine transfer ribonucleic acid: a biologically active analogue of aminoacyl transfer ribonucleic acids. Biochemistry *15*, 569-575.

Kanamori, T., Nishikawa, S., Shin, I., Schultz, P.G., and Endo, T. (1999). Uncoupling of transfer of the presequence and unfolding of the mature domain in precursor translocation across the mitochondrial outer membrane. Proc Natl Acad Sci U S A *96*, 3634-3639.

Kenner, R. A., and Aboderin, A. A. (1971). A new fluorescent probe for protein and nucleoprotein conformation. Binding of 7-(p-methoxybenzylamino)-4-nitrobenzoxadiazole to bovine trypsinogen and bacterial ribosomes. Biochemistry *10*, 4433-4440.

Kerscher, O., Holder, J., Srinivasan, M., Leung, R. S., and Jensen, R. E. (1997). The Tim54p-Tim22p complex mediates insertion of proteins into the mitochondrial inner membrane. J Cell Biol *139*, 1663-1675.

Kerscher, O., Sepuri, N. B., and Jensen, R. E. (2000). Tim18p is a new component of the Tim54p-Tim22p translocon in the mitochondrial inner membrane. Mol Biol Cell *11*, 103-116.

Kiebler, M., Pfaller, R., Sollner, T., Griffiths, G., Horstmann, H., Pfanner, N., and Neupert, W. (1990). Identification of a mitochondrial receptor complex required for recognition and membrane insertion of precursor proteins. Nature *348*, 610-616.

Koehler, C. M. (2004). New developments in mitochondrial assembly. Annu Rev Cell Dev Biol *20*, 309-335.

Koehler, C. M., Jarosch, E., Tokatlidis, K., Schmid, K., Schweyen, R. J., and Schatz, G. (1998). Import of mitochondrial carriers mediated by essential proteins of the intermembrane space. Science *279*, 369-373.

Koehler, C. M., Merchant, S., Oppliger, W., Schmid, K., Jarosch, E., Dolfini, L., Junne, T., Schatz, G., and Tokatlidis, K. (1998). Tim9p, an essential partner subunit of Tim10p for the import of mitochondrial carrier proteins. EMBO J *17*, 6477-6486.

Koehler, C. M., Murphy, M. P., Bally, N. A., Leuenberger, D., Oppliger, W., Dolfini, L., Junne, T., Schatz, G., and Or, E. (2000). Tim18p, a new subunit of the TIM22 complex that mediates insertion of imported proteins into the yeast mitochondrial inner membrane. Mol Cell Biol *20*, 1187-1193.

Kovermann, P., Truscott, K. N., Guiard, B., Rehling, P., Sepuri, N. B., Muller, H., Jensen, R. E., Wagner, R., and Pfanner, N. (2002). Tim22, the essential core of the mitochondrial protein insertion complex, forms a voltage-activated and signal-gated channel. Mol Cell *9*, 363-373.

Kozany, C., Mokranjac, D., Sichting, M., Neupert, W., and Hell, K. (2004). The J domain-related cochaperone Tim16 is a constituent of the mitochondrial TIM23 preprotein translocase. Nat Struct Mol Biol *11*, 234-241.

Kozjak, V., Wiedemann, N., Milenkovic, D., Lohaus, C., Meyer, H. E., Guiard, B., Meisinger, C., and Pfanner, N. (2003). An essential role of Sam50 in the protein sorting and assembly machinery of the mitochondrial outer membrane. J Biol Chem *278*, 48520-48523.

Krieg, U. C., Johnson, A. E., and Walter, P. (1989). Protein translocation across the endoplasmic reticulum membrane: identification by photocross-linking of a 39-kD integral membrane glycoprotein as part of a putative translocation tunnel. J Cell Biol *109*, 2033-2043.

Krieg, U. C., Walter, P., and Johnson, A. E. (1986). Photocrosslinking of the signal sequence of nascent preprolactin to the 54-kilodalton polypeptide of the signal recognition particle. Proc Natl Acad Sci U S A *83*, 8604-8608.

Kunkele, K. P., Heins, S., Dembowski, M., Nargang, F. E., Benz, R., Thieffry, M., Walz, J., Lill, R., Nussberger, S., and Neupert, W. (1998a). The preprotein translocation channel of the outer membrane of mitochondria. Cell *93*, 1009-1019.

Kunkele, K. P., Juin, P., Pompa, C., Nargang, F. E., Henry, J. P., Neupert, W., Lill, R., and Thieffry, M. (1998b). The isolated complex of the translocase of the outer membrane of mitochondria. Characterization of the cation-selective and voltage-gated preprotein-conducting pore. J Biol Chem *273*, 31032-31039.

Liu, Q., D'Silva, P., Walter, W., Marszalek, J., and Craig, E. A. (2003). Regulated cycling of mitochondrial Hsp70 at the protein import channel. Science *300*, 139-141.

Luciano, P., and Geli, V. (1996). The mitochondrial processing peptidase: function and specificity. Experientia *52*, 1077-1082.

Lutz, T., Neupert, W., and Herrmann, J. M. (2003). Import of small Tim proteins into the mitochondrial intermembrane space. EMBO J *22*, 4400-4408.

Maarse, A. C., Blom, J., Keil, P., Pfanner, N., and Meijer, M. (1994). Identification of the essential yeast protein MIM17, an integral mitochondrial inner membrane protein involved in protein import. FEBS Lett *349*, 215-221.

Martin, J., Mahlke, K., and Pfanner, N. (1991). Role of an energized inner membrane in mitochondrial protein import. Delta psi drives the movement of presequences. J Biol Chem *266*, 18051-18057.

Merlin, A., Voos, W., Maarse, A. C., Meijer, M., Pfanner, N., and Rassow, J. (1999). The J-related segment of tim44 is essential for cell viability: a mutant Tim44 remains in the mitochondrial import site, but inefficiently recruits mtHsp70 and impairs protein translocation. J Cell Biol *145*, 961-972.

Mesecke, N., Terziyska, N., Kozany, C., Baumann, F., Neupert, W., Hell, K., and Herrmann, J. M. (2005). A disulfide relay system in the intermembrane space of mitochondria that mediates protein import. Cell *121*, 1059-1069.

Mokranjac, D., Paschen, S. A., Kozany, C., Prokisch, H., Hoppins, S. C., Nargang, F. E., Neupert, W., and Hell, K. (2003). Tim50, a novel component of the TIM23 preprotein translocase of mitochondria. EMBO J *22*, 816-825.

Mokranjac, D., Popov-Celeketic, D., Hell, K., and Neupert, W. (2005). Role of tim21 in mitochondrial translocation contact sites. J Biol Chem *280*, 23437-23440.

Moro, F., Okamoto, K., Donzeau, M., Neupert, W., and Brunner, M. (2002). Mitochondrial protein import: molecular basis of the ATP-dependent interaction of MtHsp70 with Tim44. J Biol Chem *277*, 6874-6880.

Murcha, M. W., Elhafez, D., Millar, A. H., and Whelan, J. (2005). The C-terminal region of TIM17 links the outer and inner mitochondrial membranes in *Arabidopsis* and is essential for protein import. J Biol Chem *280*, 16476-16483.

Naoe, M., Ohwa, Y., Ishikawa, D., Ohshima, C., Nishikawa, S., Yamamoto, H., and Endo, T. (2004). Identification of Tim40 that mediates protein sorting to the mitochondrial intermembrane space. J Biol Chem *279*, 47815-47821.

Nargang, F. E., Preuss, M., Neupert, W., and Herrmann, J. M. (2002). The Oxa1 protein forms a homooligomeric complex and is an essential part of the mitochondrial export translocase in *Neurospora crassa*. J Biol Chem *277*, 12846-12853.

Nargang, F. E., Rapaport, D., Ritzel, R. G., Neupert, W., and Lill, R. (1998). Role of the negative charges in the cytosolic domain of TOM22 in the import of precursor proteins into mitochondria. Mol Cell Biol *18*, 3173-3181.

Neupert, W., and Brunner, M. (2002). The protein import motor of mitochondria. Nat Rev Mol Cell Biol *3*, 555-565.

Nunnari, J., Fox, T. D., and Walter, P. (1993). A mitochondrial protease with two catalytic subunits of nonoverlapping specificities. Science *262*, 1997-2004.

Paschen, S. A., Rothbauer, U., Kaldi, K., Bauer, M. F., Neupert, W., and Brunner, M. (2000). The role of the TIM8-13 complex in the import of Tim23 into mitochondria. EMBO J *19*, 6392-6400.

Paschen, S. A., Waizenegger, T., Stan, T., Preuss, M., Cyrklaff, M., Hell, K., Rapaport, D., and Neupert, W. (2003). Evolutionary conservation of biogenesis of beta-barrel membrane proteins. Nature *426*, 862-866.

Pfanner, N., Hoeben, P., Tropschug, M., and Neupert, W. (1987a). The carboxyl-terminal two-thirds of the ADP/ATP carrier polypeptide contains sufficient information to direct translocation into mitochondria. J Biol Chem *262*, 14851-14854.

Pfanner, N., Muller, H. K., Harmey, M. A., and Neupert, W. (1987b). Mitochondrial protein import: involvement of the mature part of a cleavable precursor protein in the binding to receptor sites. EMBO J *6*, 3449-3454.

Pfanner, N., and Neupert, W. (1985). Transport of proteins into mitochondria: a potassium diffusion potential is able to drive the import of ADP/ATP carrier. EMBO J *4*, 2819-2825.

Pfanner, N., and Neupert, W. (1987). Distinct steps in the import of ADP/ATP carrier into mitochondria. J Biol Chem *262*, 7528-7536.

Rapaport, D., Mayer, A., Neupert, W., and Lill, R. (1998). cis and trans sites of the TOM complex of mitochondria in unfolding and initial translocation of preproteins. J Biol Chem *273*, 8806-8813.

Rehling, P., Model, K., Brandner, K., Kovermann, P., Sickmann, A., Meyer, H. E., Kuhlbrandt, W., Wagner, R., Truscott, K. N., and Pfanner, N. (2003). Protein insertion into the mitochondrial inner membrane by a twin-pore translocase. Science *299*, 1747-1751.

Roise, D., Theiler, F., Horvath, S. J., Tomich, J. M., Richards, J. H., Allison, D. S., and Schatz, G. (1988). Amphiphilicity is essential for mitochondrial presequence function. EMBO J *7*, 649-653.

Ryan, K. R., Menold, M. M., Garrett, S., and Jensen, R. E. (1994). SMS1, a high-copy suppressor of the yeast mas6 mutant, encodes an essential inner membrane protein required for mitochondrial protein import. Mol Biol Cell *5*, 529-538.

Schatz, G. (1996). The protein import system of mitochondria. J Biol Chem *271*, 31763-31766.

Schmitt, S., Ahting, U., Eichacker, L., Granvogl, B., Go, N. E., Nargang, F. E., Neupert, W., and Nussberger, S. (2005). Role of Tom5 in maintaining the structural stability of the TOM complex of mitochondria. J Biol Chem *280*, 14499-14506.

Schneider, H., Sollner, T., Dietmeier, K., Eckerskorn, C., Lottspeich, F., Trulzsch, B., Neupert, W., and Pfanner, N. (1991). Targeting of the master receptor MOM19 to mitochondria. Science *254*, 1659-1662.

Schneider, H. C., Berthold, J., Bauer, M. F., Dietmeier, K., Guiard, B., Brunner, M., and Neupert, W. (1994). Mitochondrial Hsp70/MIM44 complex facilitates protein import. Nature *371*, 768-774.

Schwartz, M. P., and Matouschek, A. (1999). The dimensions of the protein import channels in the outer and inner mitochondrial membranes. Proc Natl Acad Sci U S A *96*, 13086-13090.

Sickmann, A., Reinders, J., Wagner, Y., Joppich, C., Zahedi, R., Meyer, H. E., Schonfisch, B., Perschil, I., Chacinska, A., Guiard, B.*, et al.* (2003). The proteome of *Saccharomyces cerevisiae* mitochondria. Proc Natl Acad Sci U S A *100*, 13207-13212.

Sirrenberg, C., Bauer, M. F., Guiard, B., Neupert, W., and Brunner, M. (1996). Import of carrier proteins into the mitochondrial inner membrane mediated by Tim22. Nature *384*, 582-585.

Sirrenberg, C., Endres, M., Folsch, H., Stuart, R. A., Neupert, W., and Brunner, M. (1998). Carrier protein import into mitochondria mediated by the intermembrane proteins Tim10/Mrs11 and Tim12/Mrs5. Nature *391*, 912-915.

Sirrenberg, C., Endres, M., Folsch, H., Stuart, R. A., Neupert, W., and Brunner, M. (1998). Carrier protein import into mitochondria mediated by the intermembrane proteins Tim10/Mrs11 and Tim12/Mrs5. Nature *391*, 912-915.

Sollner, T., Rassow, J., Wiedmann, M., Schlossmann, J., Keil, P., Neupert, W., and Pfanner, N. (1992). Mapping of the protein import machinery in the mitochondrial outer membrane by crosslinking of translocation intermediates. Nature *355*, 84-87.

Strub, A., Rottgers, K., and Voos, W. (2002). The Hsp70 peptide-binding domain determines the interaction of the ATPase domain with Tim44 in mitochondria. EMBO J *21*, 2626-2635.

Stuart, R. (2002). Insertion of proteins into the inner membrane of mitochondria: the role of the Oxa1 complex. Biochim Biophys Acta *1592*, 79.

Truscott, K. N., and Pfanner, N. (1999). Import of carrier proteins into mitochondria. Biological Chemistry *380*, 1151-1156.

Terziyska, N., Lutz, T., Kozany, C., Mokranjac, D., Mesecke, N., Neupert, W., Herrmann, J. M., and Hell, K. (2005). Mia40, a novel factor for protein import into the intermembrane space of mitochondria is able to bind metal ions. FEBS Lett *579*, 179-184.

Truscott, K. N., Kovermann, P., Geissler, A., Merlin, A., Meijer, M., Driessen, A. J., Rassow, J., Pfanner, N., and Wagner, R. (2001). A presequence- and voltage-sensitive channel of the mitochondrial preprotein translocase formed by Tim23. Nat Struct Biol *8*, 1074-1082.

Truscott, K. N., Voos, W., Frazier, A. E., Lind, M., Li, Y., Geissler, A., Dudek, J., Muller, H., Sickmann, A., Meyer, H. E.*, et al.* (2003). A J-protein is an essential subunit of the presequence translocase-associated protein import motor of mitochondria. J Cell Biol *163*, 707-713.

Tzagoloff, A. (1982). Mitochondria (New York: Plenum Press).

Ungermann, C., Guiard, B., Neupert, W., and Cyr, D. M. (1996). The delta psi- and Hsp70/MIM44-dependent reaction cycle driving early steps of protein import into mitochondria. EMBO J *15*, 735-744.

Ungermann, C., Neupert, W., and Cyr, D. M. (1994). The role of Hsp70 in conferring unidirectionality on protein translocation into mitochondria. Science *266*, 1250-1253.

van der Laan, M., Chacinska, A., Lind, M., Perschil, I., Sickmann, A., Meyer, H. E., Guiard, B., Meisinger, C., Pfanner, N., and Rehling, P. (2005). Pam17 is required for architecture and translocation activity of the mitochondrial protein import motor. Mol Cell Biol *25*, 7449-7458.

Vestweber, D., Brunner, J., and Schatz, G. (1989). Modified precursor proteins as tools to study protein import into mitochondria. Biochem Soc Trans *17*, 827-828.

Voisine, C., Craig, E. A., Zufall, N., von Ahsen, O., Pfanner, N., and Voos, W. (1999). The protein import motor of mitochondria: unfolding and trapping of preproteins are distinct and separable functions of matrix Hsp70. Cell *97*, 565-574.

von Heijne, G. (1986). Mitochondrial targeting sequences may form amphiphilic helices. EMBO J *5*, 1335-1342.

Voulhoux, R., Bos, M. P., Geurtsen, J., Mols, M., and Tommassen, J. (2003). Role of a highly conserved bacterial protein in outer membrane protein assembly. Science *299*, 262-265.

Wiedemann, N., Kozjak, V., Chacinska, A., Schonfisch, B., Rospert, S., Ryan, M. T., Pfanner, N., and Meisinger, C. (2003). Machinery for protein sorting and assembly in the mitochondrial outer membrane. Nature *424*, 565-571.

Wiedemann, N., Pfanner, N., and Ryan, M. T. (2001). The three modules of ADP/ATP carrier cooperate in receptor recruitment and translocation into mitochondria. EMBO J *20*, 951-960.

Wieprecht, T., Apostolov, O., Beyermann, M., and Seelig, J. (2000). Interaction of a mitochondrial presequence with lipid membranes: role of helix formation for membrane binding and perturbation. Biochemistry *39*, 15297-15305.

Yamamoto, H., Esaki, M., Kanamori, T., Tamura, Y., Nishikawa, S., and Endo, T. (2002). Tim50 is a subunit of the TIM23 complex that links protein translocation across the outer and inner mitochondrial membranes. Cell *111*, 519-528.

Young, J. C., Hoogenraad, N. J., and Hartl, F. U. (2003). Molecular chaperones Hsp90 and Hsp70 deliver preproteins to the mitochondrial import receptor Tom70. Cell *112*, 41-50.

VITA

Name: Holly Beth Cargill

Address: Department of Biochemistry/Biophysics
c/o Dr. Arthur E. Johnson
Texas A&M University
MS 1114
College Station, TX 77843-1114

Email Address: hmcargill@tamu.edu

Education: B.S., Biochemistry, The University of Nebraska – Lincoln, 1999
M.S., Biochemistry, Texas A&M University, 2006